Preprints (www.preprints.org) | NOT PEER-REVIEWED | Posted: 13 August 2021

Article

MIS 5.5 highstand, and future sea level flooding at 2100 and 2300 in tectonically stable areas of central Mediterranean sea: Sardinia and the Pontina Plain (southern Latium), Italy

Giacomo Deiana[1-2]*, Fabrizio Antonioli[3], Lorenzo Moretti[4], Paolo E. Orrù[1-2], Giovanni Randazzo[5], Valeria Lo Presti[5]

[1] Department of Chemical and Geosciences - University of Cagliari, 09042,Italy. (G.D.) giacomo.deiana@unica.it ; (P.O.) orrup@unica.it
[2] CoNISMa – Consorzio Nazionale Interuniversitario per le Scienze del Mare, 00196 Roma, Italy.
[3] INGV Istituto di Geofisica e Vulcanologia, 00143 Rome, Italy. fabrizioantonioli2@gmail.com
[4] ENEA, 40129 Bologna, Italy; lorenzo.moretti@enea.it
[5] Department of Mathematics, Pysics and Geosciences, MIFT, University of Messina, 98166 Messina, Italy; (G.R.); grandazzo@unime.it ; (V.L.) valeria.lopresti@gmail.com ;
* Correspondence: giacomo.deiana@unica.it

Abstract: Mediterranean Sea are dynamic habitats in which human activities have been conducted for centuries and which feature micro-tidal environments with about 0.40 m of range. For this reason, human settlements are still concentrated along a narrow coastline strip, where any change in the sea level and coastal dynamics may impact anthropic activities. We analyzed light detection and ranging (LiDAR) and Copernicus Earth Observation data. Aim of this research is to provide estimates and detailed maps (in three coastal plain of Sardinia (Italy) and in the Pontina Plain (southern Latium, Italy) of: i) the past marine trasgression occurred during MIS 5.5 higstand 119 kyrss BP; ii) the coastline regression occurred during the last glacial maximum MIS 2 (21.5 krs cal BP) and iii) the potential marine submersion for 2100 and 2300. The objective of this multidisciplinary study is to provide maps of sea-level rise future scenarios using the IPCC RCP 8.5 2019 [1]projections and glacio-hydro-isostatic movements for the above selected coastal zones, which are the locations of touristic resorts, railways, and heritage sites. We estimated a potential loss of land for the above areas of between about 146 km² (IPCC 2019-RCP8.5 scenario [1]) and 637 km² along a coastline length of about 268 km.

Keywords: central Mediterranean, coastal Plains, sea level at 2100 and 2300, Sardinia, Pontina Plain

1. Introduction

Future warming on Mediterranean Sea could provide higher sea level rise than published on 2019 IPCC report [2]. Many research was recently published on the effects of sea level rise on the Mediterranean coasts [3,4,5,6]. In this research we use the methodologies tested in previous works [3] where the relative sea level is the sum of eustasy, isostasy and tectonic movement. We used the IPCC 2019 AR 8.5 projections for the sea level rise expected at 2100 [1]. The objectives of our work is to highlight at what altitude can now be observed the fossil signs of maximum marine ingression (forms and aged deposits) occurred during MIS 5.5 comparing

© 2021 by the author(s). Distributed under a Creative Commons CC BY license.

Preprints (www.preprints.org) | NOT PEER-REVIEWED | Posted: 13 August 2021

with the sea level projections for 2100 and 2300 (IPCC 2019) in the 4 coastal sites under study (Figure 1). We also take in consideration the MIS 5.5 maximum highstand comparing the observed data in field with the ice model [7] projections for Sardinia and Pontina Plain. Also, on the basis of the bathymetry and the available data and models, we positioned the 21.5 ka cal BP coastline reached during the LGM (Last Glacial maximum) on the continental shelf in front of the Plains. Furthermore, on the basis of the IPCC projections we have calculated (adding the geological vertical movements) the altitude at which the sea will be reached (according to the AR 8.5 scenario) at 2100 and 2300. We have chosen these sites because they are located in Sardinia, one of the most stable areas of the Mediterranean and in Southern Lazio, a similar stable coastal area [8] but with high rates of subsidence partly due to tectonics and partly due to the drying of the peat drained by the reclamation of the 1930s and 1940s.

An innovative methodology made for the first time for drafting the sea flooding maps, was to "look" not only to the future (2100, 2300) but also to the past. We indagated in the studied areas in order to understand what were the effects of the maximum transgression of the last highstand, (MIS 5.5 that occurred 119 ka BP), this choice is due to very specific reasons. There is a generalized belief that since the maximum insolation on Earth ceased about 6000 years ago (climatic optimum) we are “walking” towards an ice age. The duration of last warm periods (MIS 5.5, MIS 9, MIS 11, etc.), has always been around 10-11 thousand years [9]. But, if it is true that 119 ka BP there was a maximum of insolation of about 550 W\m^2, calculated for 65 ° in June, it is also true that during the climatic optimu (about 6, ka BP) l insolation was of lesser entity: 520 W\m^2. Subsequently: 1) the insolation has been decreasing, 2): the climate does not seem to have cooled). In a quoted article [10], entitled "An exceptional long Interglacial period?" The Authors show that due to a particular movement of eccentricity the "warm-hot" climatic period instead of taking us towards an ice age (as happened in the last 4 higstand on earth) should last at least another 50 ka (Figure 1) "But more recent studies point toward a different future: a long interglacial that may last another 50,000 years".

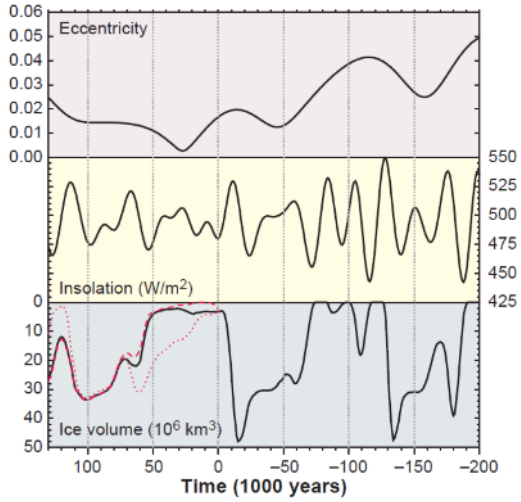

Figure 1 Long-term variations of eccentricity (top), June insolation at 65°N (middle), and simulated Northern Hemisphere ice volume (increasing downward) (bottom) for 200,000 years before the present to 130,000 from now. Time is negative in the past and positive in the future. For the future, three CO2 scenarios were used: last glacial-interglacial values (solid line), a human-induced concentration of 750 ppmv (dashed line), and a constant concentration of 210 ppmv (dotted line). Simulation results from [1,2]; eccentricity and insolation from [12].

Preprints (www.preprints.org) | NOT PEER-REVIEWED | Posted: 13 August 2021

119 ka BP the insolation was a higher than oday, the sea was about 8 meters higher [7], but the CO^2 content in the atmosphere has never exceeded 295 ppm, while today, with a lower insolation, but a content of CO^2 much higher, 415 ppm, we can also observe a sea level 8 meters lower than 119 ka BP and a rise that exceeds the acceleration of 3 mm / year. IPCC 209 projections estimates (using the RCP 8.5 scenario) a rise higher than one meter for the next 79 years (2100). The CO^2 increase would also further delay the triggering of a cold period.

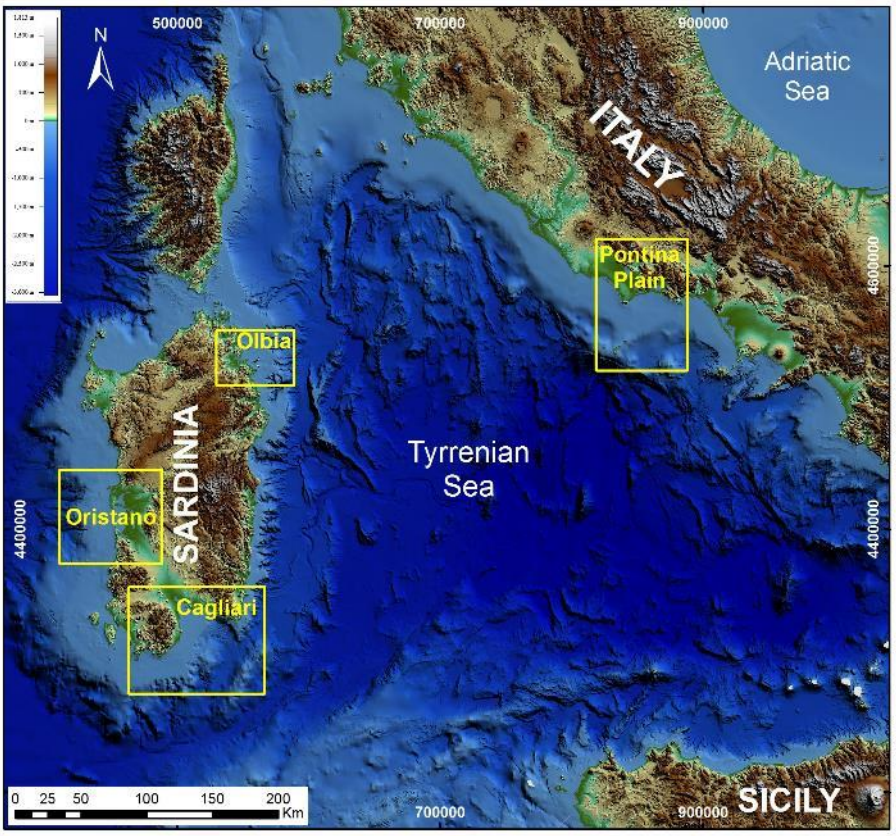

Figure 2 Overview map of the Central Mediterranean region showing the locations (red dots) of the coastal plains studied.

2. Materials and Methods

This research is based on the method described in [4], and [14], to ensure homogeneity and enable a comparison with previous results, extending the study toward other central Mediterranean coastal plains, besides Italy. Sea-level change along the Mediterranean coast is the sum of eustatic, glaciohydro-isostatic, and tectonic factors. The first is time dependent while the latter two also vary with location, consists to sum the different components of sea level rise in the following main steps: (a) the IPCC-AR5 projections (RCP-8.5 upper limits scenarios report IPCC 2019), the long term land vertical movements from geological data [7,8,15];c) the glacio-hydro-isostatic movement (GIA) [3]; (d) by combining eustatic, isostatic and tectonic data projected up to 2100, and 2300, we provided the expected sea-levels at 2100 and 2300 for the investigate coastal areas and the expected inland extent of related marine flooding. The choice of the study areas was decided by several

Preprints (www.preprints.org) | NOT PEER-REVIEWED | Posted: 13 August 2021

different factors: (i) tectonics (stable areas only); (ii) exposure, (iii) max fetch, (iv) sedimentological material, (v) wave energy flux, (vi) bedrock and (vii) geomorphological features. Our maps show the maximum sea-level height expected for 2100 and 2300 for the above reference climatic projections and the corresponding flooded area. Sea level rose rapidly between 21 until about 4 ka years ago. Over the last 100 years the sea level has risen globally by 18 cm, and by 14 cm (on average 1.4 mm /year) in Mediterranean sea, the differences between the global and a lower rise of the Mediterranean, considered a closed basin, are due to evapotranspiration and to an increasingly limited flow of rivers.

We remark that our analysis does not take into account hydrodynamics models, and the contribution of sediment flow from rivers, coastal erosion and all the possible anthropic defences that may change the estimated extension of the flooded areas proposed in this study.

2.1 Field work

2.1.1. Pontina Plain

For this Plain, some papers published in the 1930s and 1950s were carefully considered, the altitude of fossil deposit containing Persistrombus latus or Senegalese fauna, was revised also in field (respect the review [8] and [16]), lowering it from +10 to +5.3 m. In addition, some new lagoonal fossil layers containing Cerastoderma edulis have been founded in the field. These lagoonal levels outcropping in the eastern portion of Pontina plain, between +4 and -2 m, outcrops only if incised by the the 1930s "Bonfica" channels whose cleaning reveals the fossil levels. We checked what published in [17], in 3 outcrops on field. The altitudes were re-measured on google Earth maps (which presents a very precise altimetry in the flat areas see also Material and Method [14]).

2.1.2 Sardinia

As part of this work, the stratigraphic and chronological point of view of deposits containing Persististrombus latus, Patella ferruginea, etc., have been reviewed, detected in previous studies [18,19,20] at altitudes between +4.0 m and +8.0 m a.s.l. The levels containing lagoon fossils with Cerastoderma Edulis were found in the plains of Cagliari (Elmas-Assemini plane) and of Oristano (north of the Cabras lagoon). The respective elevations were determined through measurements with a DGPS antenna - Trimble R8s model. The planimetric and altimetric survey were carried out operating in static mode. The raw DGPS data have been processed using the Trimble Busines software (V. 2.50). The processed data have an accuracy of ± 1 ÷ 2 cm.

2.2 Digital terrain Models

To map the sea-level rise scenarios, a data set of high-resolution topography based on light detection and ranging (LiDAR) observations produced by dierent agencies from 2008 to 2019 was used (Table 1). The extracted Digital Terrain Models (DTM) were obtained at variable spatial resolutions depending on the data set and in the range at about 20 cm of mean vertical resolution [21]. The details of the characteristics of the DTM are described in Table 1 and in the maps available in the online supporting material.

Preprints (www.preprints.org) | NOT PEER-REVIEWED | Posted: 13 August 2021

To link the land surface to the seafloor along the coasts and represent MIS 2 sea level, the bathymetric data were obtained from European Marine Observation and Data Network (EMODnet, http://portal.emodnet-bathymetry.eu/ [22]). Marine and terrestrial topographic data were co-registered and georeferenced into the same UTM-WGS84 (Zones 32 and 33) reference frame, and the shoreline position was determined relative to the epoch of the surveys for each area. The details regarding the link to the website from which we downloaded or requested the digital data are also described in the online supporting material.

DTMs were mapped and analyzed by Global Mapper Software® (www.globalmapper.com [23]) (Version 21, Hallowell, ME, USA) to create 3D high-resolution maps of the investigated areas, on which the position of the present-day coastline and its potential position in 2100 as a result of relative sea-level rise are shown by contour lines. The DTMs with contour lines and submerged surfaces were represented using the color shaded option and exported as georeferenced images through GIS composer (Tables 1,2).

3. Results

3.1 Geomorphology and altitude of MIS 5.5 in Sardinia sites.

3.1.1. Cagliari coastal plains

The coastal sector of Campidano graben of Cagliari (Figure 2), is articulated in 2 coastal plains with different geodynamic evolution: the eastern plain is set on a graben structure active until the upper Miocene, while western plain is set on a graben active until the lower-middle Pleistocene.

Sant Elia Cape represents a closure towards the sea of the Cagliari hills horst structure, where A. Lamarmora in 1856 surveyed for the first time the Last Intergacial stratigraphic succession. Later, this stratigraphic section was indicated as locus typicus of the "Tyrsrhenian plane" [18], an attribution confirmed by U/Th isotopic dating corals [8,19,20]. Maximum sea ingression during MIS 5.5 formed two deep bays separated by the Cagliari Hills promontory and the paleo Island of Sant Elia and Sella del Diavolo reliefs. Afterwards, sedimentation from two tributary rivers (Rio Mannu-Cixerri to the West and Riu Saliu and Cungiaus to the East) led to the emersion of the Sa Illetta barrier islands forming the actual Santa Gilla Lagoon (West sector) and to the formation of Is Arenas littoral spit closed the Molentargius paleo-lagoon (East sector). Evidence of the shoreline of MIS 5.5 maximum ingression was reported by Segre [24], in the Elmas coastal plain, behind the innermost part of Santa Gilla Lagoon, represented by coastal gravel deposit in a fossiliferous sandy matrix of Cerastoderma glaucum.

During observations for the study of the Holocene sea rise, the site described by Segre [24] and Orrù [25] was detected; in the present work, the inner margin of the MIS 5 transgression was recognized in both Santa Gilla and Molentargius coastal plains, represented by an bank erosion incised in Middle Pleistocene alluvial deposits (MIS 6?) on which they rest in onlap.

The MIS 5 marine-littoral depositional terraces are composed by predominantly quartzose gravels at the elevation of +3.8 m in the western sector (Elmas-Assemini plain)

Preprints (www.preprints.org) | NOT PEER-REVIEWED | Posted: 13 August 2021

N	A Site	b DTM Resolution ± Vertical accu-racy (m)	c Map year	d Projection 2100 IPCC 2019 AR 8.5, Upper likely range mm	e Projection 2100 IPCC 2019 AR 8.5, Median range mm	f Projection 2300 IPCC 2019 AR 8.5, Upper likely range mm	g Projection 2300 IPCC 2019 AR 8.5, Median range mm	h GIA mm\y	i Vertical Movemnts mm\y	l Total mm IPCC 2100 Upper likely range	m Total mm IPCC 2100 Median range	n Total mm IPCC 2300 Upper likely range	o Total mm IPCC 2300 Median range
1	Cagliari	LIDAR 5x5 (±0.2)	2008	1100	840	5200	3700	0,57	-	1152	893	5252	3752
2	Oristano	LIDAR 1x1 (±0.2)	2008	1100	840	5200	3700	0,57	-	1152	893	5252	3752
3	Olbia	LIDAR 1x1 (±0.2)	2008	1100	840	5200	3700	0,62	-	1157	897	5256	3756
4	Pontina	25x25 ±1	2010	1100	840	5200	3700	0,44	-0.1	1149	889	5249	3749

Table 1. **a**: site; **b**: (digital terrain model, DTM) resolution and accuracy; **c**: epoch of DTM; **d,e,f,g**: IPCC projection AR5-RCP8. **h** : glacial isostatic adjustment (GIA) rate [3]; **i**: vertical tectonic rate mm/year; **l,m,n,o**: relative sea-level rise for 2100, 2300, IPCC AR5-RCP 8.5 scenario.

Preprints (www.preprints.org) | NOT PEER-REVIEWED | Posted: 13 August 2021

Table 2 Modelled and observed altitude during Lgm (21.5 kyrss cal BP) and MIS 5.5 (119 yrs BP)

Sites	Altitude Lgm – model, [3]. m	Altitude Lgm Model, [26]. m	Observed Lgm altitude	Altitude MIS 5.5 Model, [7]. m	Observed MIS 5.5 altitude. M This paper
Cagliari	-129.2	-122	-125	+8.4	+4.8
Oristano	-126.8	-124	-130	+8.6	+6.5
Olbia	-127.5	-122	-126	+8.5	+4.9
Pontina	-117,8	-117	-----	+8.2	+7.96, -12

(Figure 3 and Figura 4 - Section 5) and of fossiliferous sandstones with inclined lamination at the maximum elevation of 4.80 for the eastern sector (Pirri-Monserrato plain) (Figure 4 - Section 4); the lower elevation of the Elmas marine terrace could be related to the greater incidence of the western plain subsidence, as hosted in a structure with recent tectonic activity.

The paleo barrier island of Sa Illetta has a maximum elevation of MIS 5 littoral deposits at + 4.30 m in correspondence with a bioconstructed reef with corals (Cladocora coespitosa) and red algal associations of Litophyllum [27] (Fig. 4 - Section 2). Comparative U/Th and aminostratigraphic analyses on corals have attributed an age of - 149 10 kyrs BP [20]); Similar chronostratigraphic placement based on ESR analyses on Arca noae [28] present littoral deposits of the Is Arenas paleo-beach that reach a maximum aqltitude of + 4.5 m (Fig. 4 - Section 3).

During the excavation of the access channel to the Container Port of Cagliari, a tanatocenosis of Persististrombus latus -10 m was sampled (Fig. 4 - Section 1). We describe in this paper a new section of the same level at -16,50 m, analysed during dive survey in the deepening area of the outer channel.

Geophysical surveys (seismic profile, [25]) allowed to follow the paleo-valleys (mostly buried) carved during the MIS 2, these cross the whole platform until they reach the shelf break where contribute to the construction of low stationing terraces (LGM palaeo-sealevels); sometimes are involved in mass gravitational movements [29].

A Punic paleo-sea level (2500 BP) buried at -2 m is preserved in the innermost area of the Santa Gilla lagoon [30,31,32].

Preprints (www.preprints.org) | NOT PEER-REVIEWED | Posted: 13 August 2021

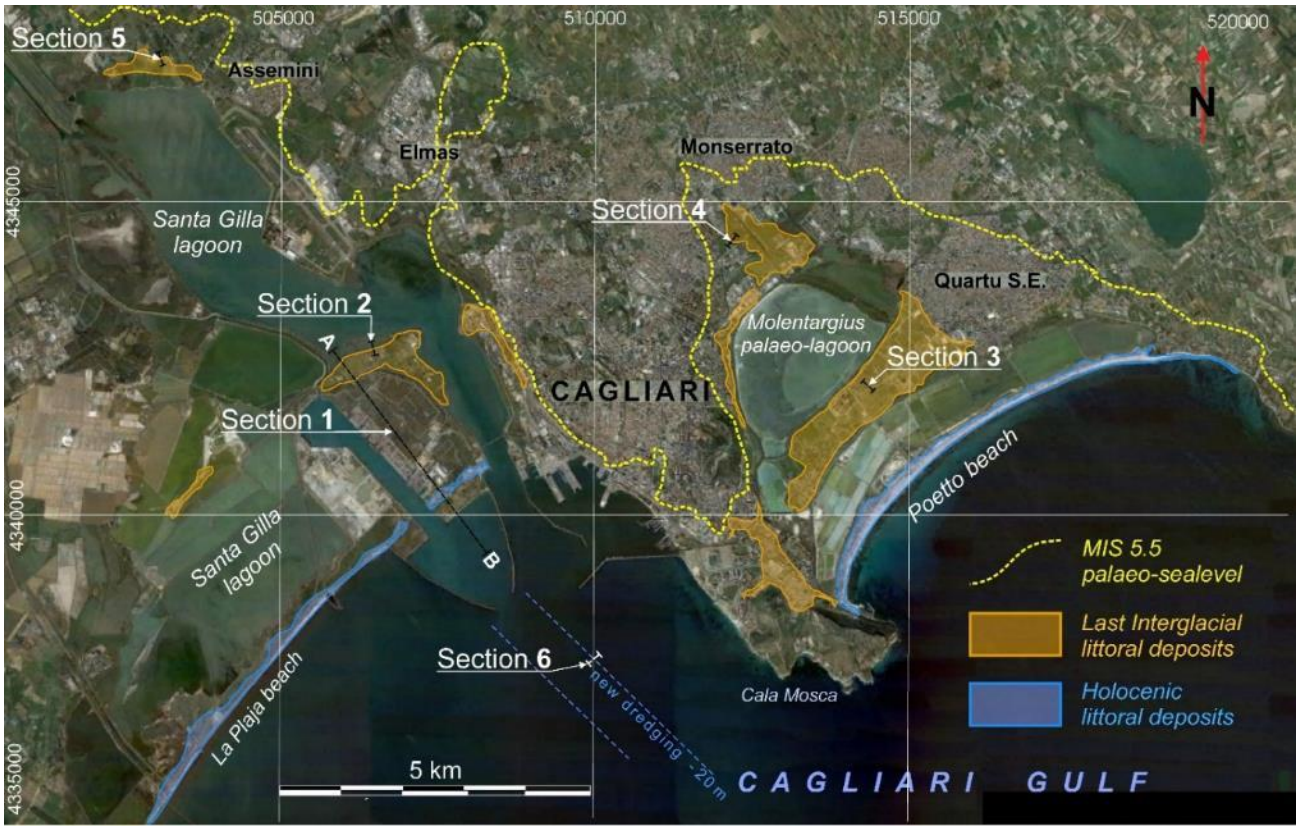

Figure 3 Aerial photograph of the coastal plain of Cagliari showing the main geomorphological features, yellow dashed line indicates the palaeo high sea level of MIS 5.5 "Tirreniano"; the littoral deposits of Last Interglacial (LI) and the Holocenic shore deposits. Location of MIS5 stratigraphic sections: **Section1**, geological profile crosses the container port for 4 km; **Section 2**, the north face of a large palaeo barrier island of the MIS 5.5 of Sa Illetta in front of Santa Gilla Lagoon [20]; **Section 3**, located in a quarry in the littoral paleo spit of Is Arenas; **Section 4** e **5** marine terraces at the inner margin of theMIS 5.5transgression overlapping fluvial deposits of MIS 6; **Section 6** MIS5 deposits intercepted from the dredging embankment at - 16.5 m, 4 meters below in the seabed.

Preprints (www.preprints.org) | NOT PEER-REVIEWED | Posted: 13 August 2021

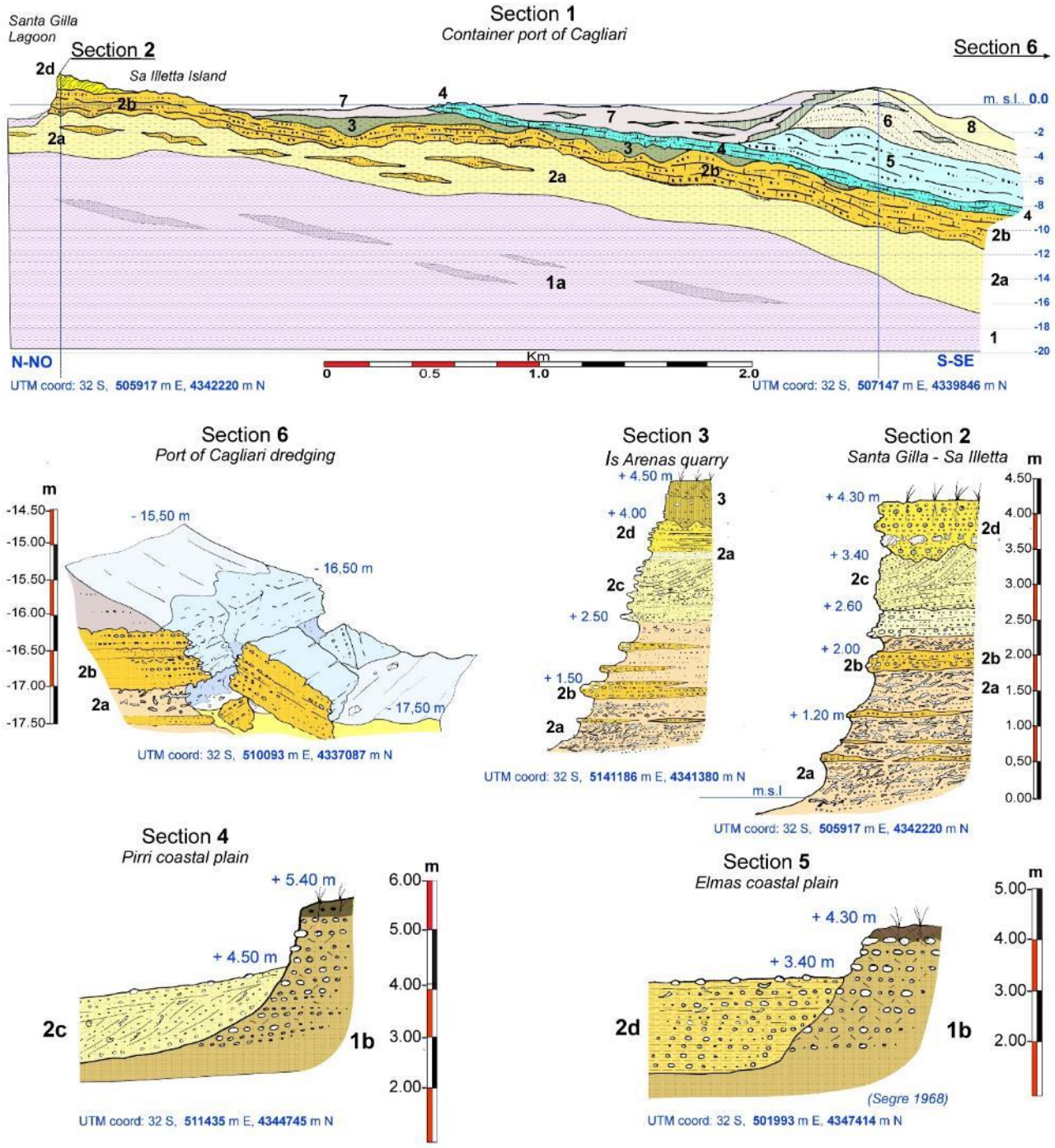

Figure 4 Stratigraphic sections of theMIS 5.5sequences in the Cagliari coastl plain. **1a**) (Section 1) deltaic complex in silt and sandy silt with clay and sand with *Ostrea sp.* in lenses (MIS 6); **1b**) (Sections 4/5) fluvial deposit with polygenic and heterometric pebbles in oxidized clayey silt matrix, weakly cemented (MIS 6); **2a**) mainly sandy littoral deposit irregularly cemented with burrows bioturbation structures, containing *Persistisstrombus latus* e *Cerastoderma glaucum* (MIS 5); **2b**) mainly quartz conglomerates and microconglomerates, fossiferous with plane-parallel lamination (MIS5); **2c**) polygenic gravels and sands alternating with fossiliferous horizons, to inclined lamination and foresets (MIS 5); **2d**) bioclastic sandstone in *Lithtaminium* and bioconstructions in *Cladocora coespitosa*; **3a**) limi sabbiosi palustri (MIS 4/2); **3b**) silty sands with pulmonate gastropods (MIS 4/2); **4**) bioclastic sandstone in *Cerastoderna sp* (Holocene); **5**) polygenic gravel with sandy matrix (Holocene); **6**) littoral sands and gravels (Holocene); **7**) silty sands lagoon deposits with interbedded peat in *Posidonia oceanica* (Present); **8**) sandy littoral deposits (Present).

Preprints (www.preprints.org) | NOT PEER-REVIEWED | Posted: 13 August 2021

Figure 5 a) a view of the section of Sa Illetta marine interglacial fossiliferous sediments [8]; tidal plain sandy littoral deposit irregularly cemented with burrows bioturbation structures and plane-parallel lamination (Section 1-2); **b**) section 2 bottom - 2a, particular of the icnofacias due to the activity of *Polychaetes;* **c**) section 2 top – 2d, bioclastic sandstone well cemented containing *Lithtaminium* and bioconstructions in *Cladocora coespitosa* - 149 ± 10 kyrs BP [20]; **d**) a view of the section of the Last Interglacial interdidal fossiliferous sediments of Is Arenas Sa (Section 3 – 2a) bottom level with burrows bioturbation structures containing *Persististrombus latus* [20]; **e**) at the top conglomeratic heterometric and polygenic fossiliferous level (Section 3 – 2b), at the bottom weakly cemented sandstones and sands with channeled flow structures in a tidal plane environment (Section 3 – 2a); **f**) sub-horizontal laminated sandstone enclosing a forest level containing *Arca Noae Limne, Arca tetragona tetragona Poli, Glycimeris sp*. 111 kyrs BP [28].

Preprints (www.preprints.org) | NOT PEER-REVIEWED | Posted: 13 August 2021

3.1.2 Oristano North coastal plains and Sinis peninsula

An extensive Wave-cut platform, incised in middle Miocene marlstone and upper Pliocene basalts, was detected in the eastern coast of Capo San Marco (southern part of the Sinis peninsula). Littoral deposit of MIS 5.5 is set on the platform, represented by a heterometric conlomerate with large basaltic blocks at the base, followed by micronglomerates and plane-parallel lamination fossiliferous sandstone with *Persististrombus latus, Patella ferruginea, Mytilus galloprovincialis* up to the altitude of +4.5 m [33]. The inner margin, generally hidden by MIS 5.5 littoral sediments and the overlying eolianites (MIS 4-2), is observable in the southernmost part of Capo San Marco at +6.5 m.

The MIS 5.5 marine-littoral deposits sequence is most preserved along the western coast of San Giovanni di Sinis [34]. The sequence (Fig. 8 - Section 1) is interrupted by erosion surfaces incised into the continental aeolian and colluvial deposits containing vertebrate and gastropod pulmonate remains from MIS 6. The transgressive succession is characterized from the base by polygenic erometric conglomerates, passing to fossiliferous quartz microconglomerates and fossiliferous sandstones (*Arca noae, Mytilus galloprovincialis, Spondylus gaederopus, Patella ferruginea, Thai haemastoma, Dentalium sp*) with plane-parallel and inclined lamination.

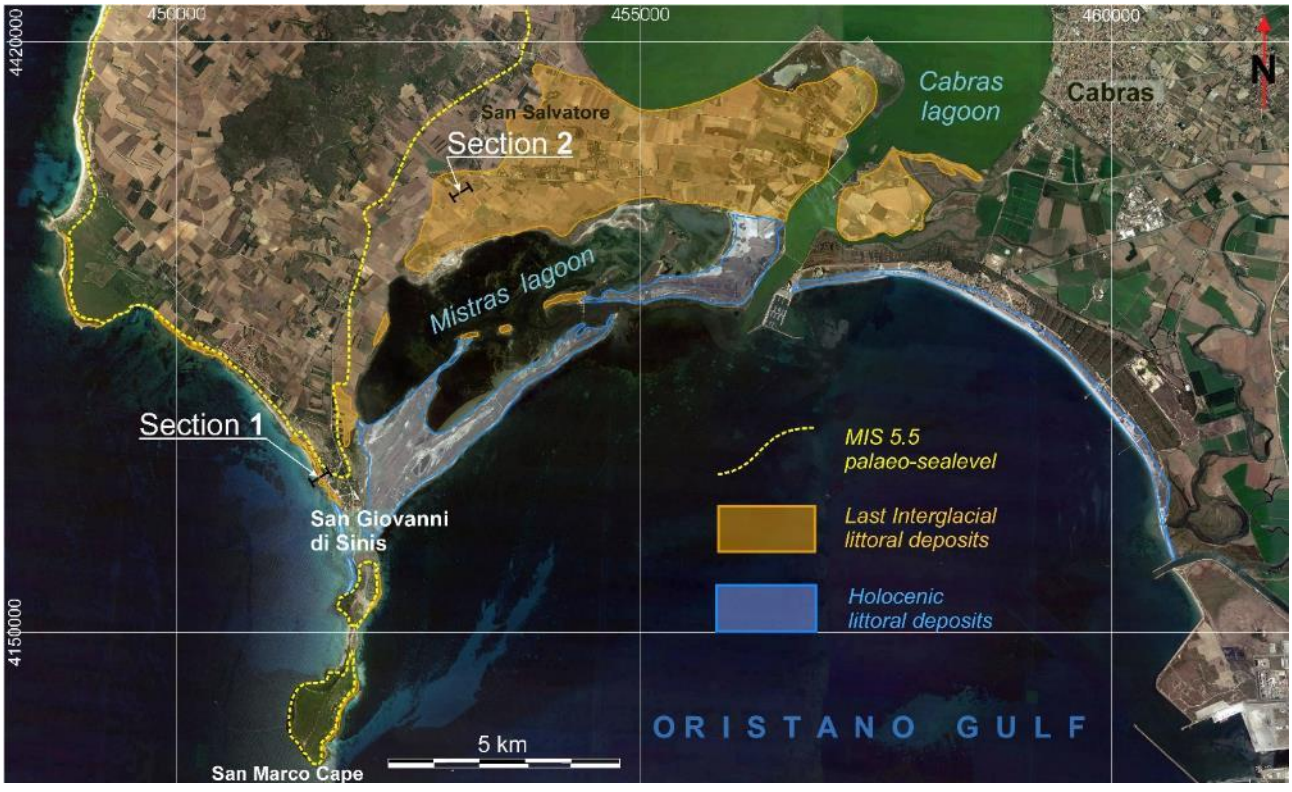

Figure 6 - Aerial photograph of the coastal plain north of Oristano and Sinis Peninsula showing the main geomorphological features, yellow dashed line indicates the palaeo high sea level of MIS 5.5; the littoral deposits of Last Interglacial (LI) and the Holocenic shore deposits. Location of MIS5 stratigraphic sections (Fig. 8): **Section1** on the rocky coast of San Giovanni, Sinis peninsula; **Section 2**, on a Punic quarry located in the Cabras palaeo littoral barrier of MIS 5.

Preprints (www.preprints.org) | NOT PEER-REVIEWED | Posted: 13 August 2021

The continuity of the sequence is interrupted by numerous erosion surfaces that sometimes retain levels or pockets of sandy paleosols with a strongly oxidized matrix. At the top o, theMIS 5.5sequence is sealed by continental deposits with sandy colluvium and Aeolian sandstone cross lamination (MIS 4-2).

The palaeo-litoral bar of theMIS 5.5that closes the Cabras Lagoon is made up of flat-parallel and inclined sandstones that include foreset structures. The summit depositional surface of the MIS 5 deposits is located at altitudes between + 4.30 and + 4.50 m (Figure 8 - Section 2), The significant sections are revealed on the walls of irrigation canals and of an ancient Punic-Roman quarries between Cabras and San Salvatore. The inner margin of the maximum marine ingression of MIS 5.5 is masked by slope deposits and river sediments from the Holocene.

Preprints (www.preprints.org) | NOT PEER-REVIEWED | Posted: 13 August 2021

Figure 7 – a) DGPS measurements of the stratigraphic section of the Pleistocene deposits of San Giovanni of Sinis; **b**) a view of the section of San Giovanni Stratigraphic showing continental deposits of the Middle Pleistocene and deposits of the Last Interglacial fossilized by regression aeolian sediments [8,33,34] (Fig. 8); **c**) particular of the organogenic level composed exclusively of valves of *Mitilus galloprovincialis* (MIS5); **d**) excavation surface of the Phoenician-Punic quarry (2500 yrs BP) engraved in theMIS 5.5beach sandstones in the palaeo-littoral spit of Cabras; **e**) detail showing the plane-parallel laminations that enclose a foreset level.

Preprints (www.preprints.org) | NOT PEER-REVIEWED | Posted: 13 August 2021

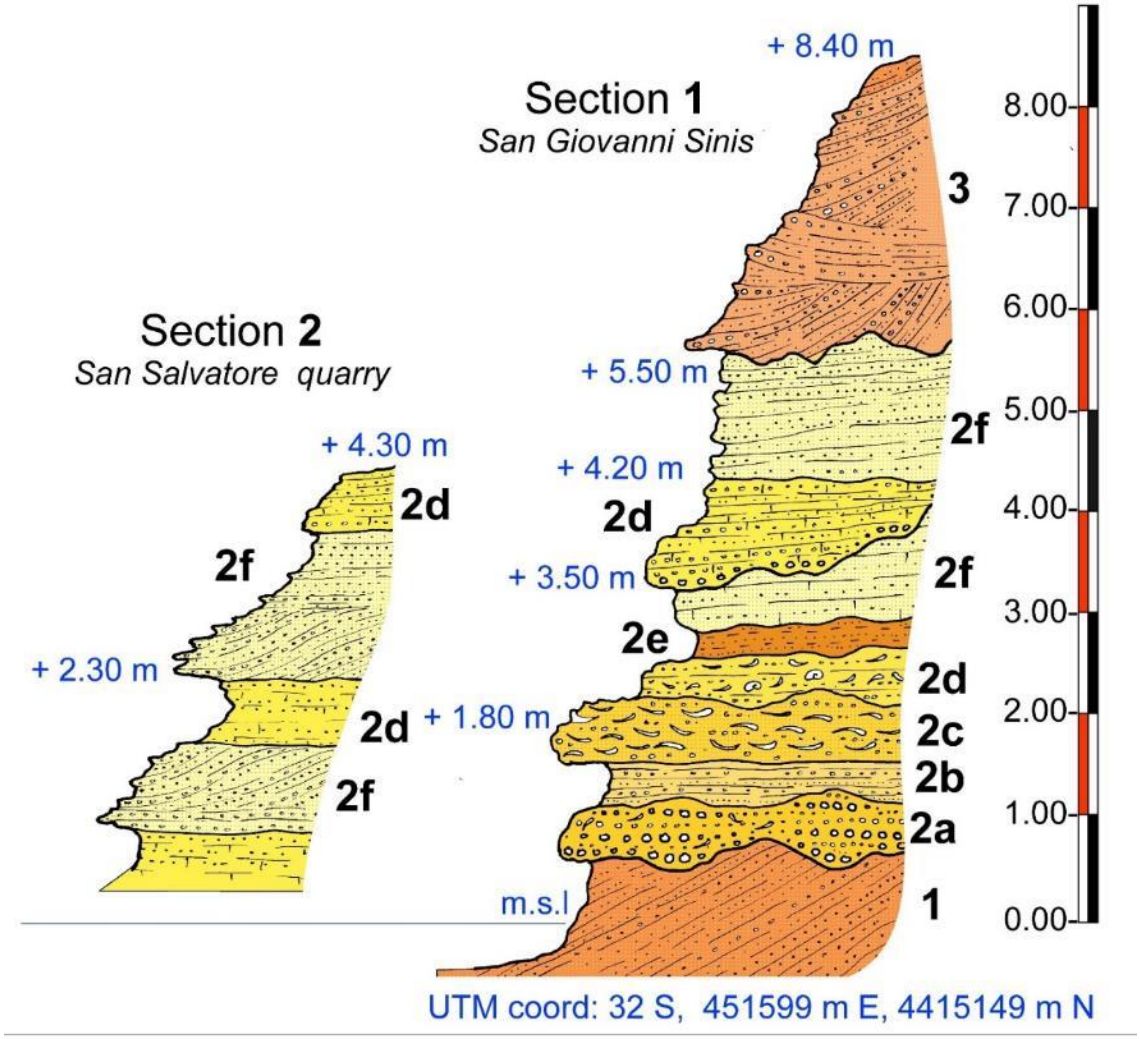

Figure 8 - Stratigraphic sections of the Medium-Upper Pleistocene sequences in Oristano North coastal plain and in Sinis peninsula. **1**) (Section 1) Aeolian sandstones with inclined layering laminae containing vertebrate remains (MIS6); **2a**) polygenic heterometric conglomerate with a fossiliferous arenaceous matrix (MIS5); **2b**) sandstones and micro-conglomerates mainly quartz with carbonate cement (MIS5); **2c**) almost exclusively organogenic level in Mitilus galloprovincialis (MIS5); **2d**) fossiliferous conglomerate and microconglomerates with a well cemented arenaceous matrix (MIS 5); **2e**) sandy palaeosoil with a strongly oxidized matrix, Munsell 5YRS 5/8;; **2f**) planar-parallel lamination sandstones alternating with foreset levels (MIS5); **3**) cross-laminated aeolian sandstones containing foraminifera and gastropods pulmonata Helicidae (MIS 4?) [33,34].

3.1.3 Olbia gulf and coastal plains

Preprints (www.preprints.org) | NOT PEER-REVIEWED | Posted: 13 August 2021

MIS 5.5 deposits in the Olbia Gulf were first described by Segre [35], which indicated extensive outcrops of conglomerates and fossiliferous sandstones along the northern coast of Golfo Aranci and along the southern coast of Tavolara Island in front of Spalmatore Bay.

Here, the transgressive level with large heterometric blocks both crystalline and carbonate rocks, fossilizes the wave-cut platform set on inequigranular Leucogranites. This basal level is covered by a well-cemented biogenic calcarenite with high fossil content (Conus mediterraneus, Conus vayssieri, Hexaplex trunculus, Cerithium vulgatum, Cerithium rupestre, Bittium reticulatum, Thais haemastoma, Columbella rustica, Arca noae, Barbatia barbata, Spondylus gaederopontaus, Patella ferruginea, Chama gryphina, Venus verrucosa, Chamelea gallina and Tapes sp.) [36].

The marine-littoral sediment sequence is organized at levels and lenses of coarse gravels, alternating with fine-grained sediments up to a maximum height of + 5.5 m (Fig. 11 - Section 1). MIS 5.5 deposits are sealed upward by strongly cemented continental landslide deposits (MIS 4?).

The sedimentary sequence of MIS 5.5at Punta La Mandria, have of lower thickness and rests discordantly on both Paleozoic granitoid substrate and Middle Jurassic arenaceous dolomitic limestone. The succession is fossilized by both rockfalls and cryoclast deposits represented by alternating Eboulis ordonnés and Grezes litees (LGM).

Data about the elevation of tidal notches incised during the MIS 5.5 higth stand are presented. The elevations (Fig 11 - tab. 2) show a relative tectonic stability of the area, but a slight negative tilting, di ffering the elevations of the southern cliff to the northern cliff of Tavolara Island. This tendency is more marked towards Capo Figari.

Similar movements, although of greater magnitude, have been found in the Gulf of Orosei and Capo Caccia [7].

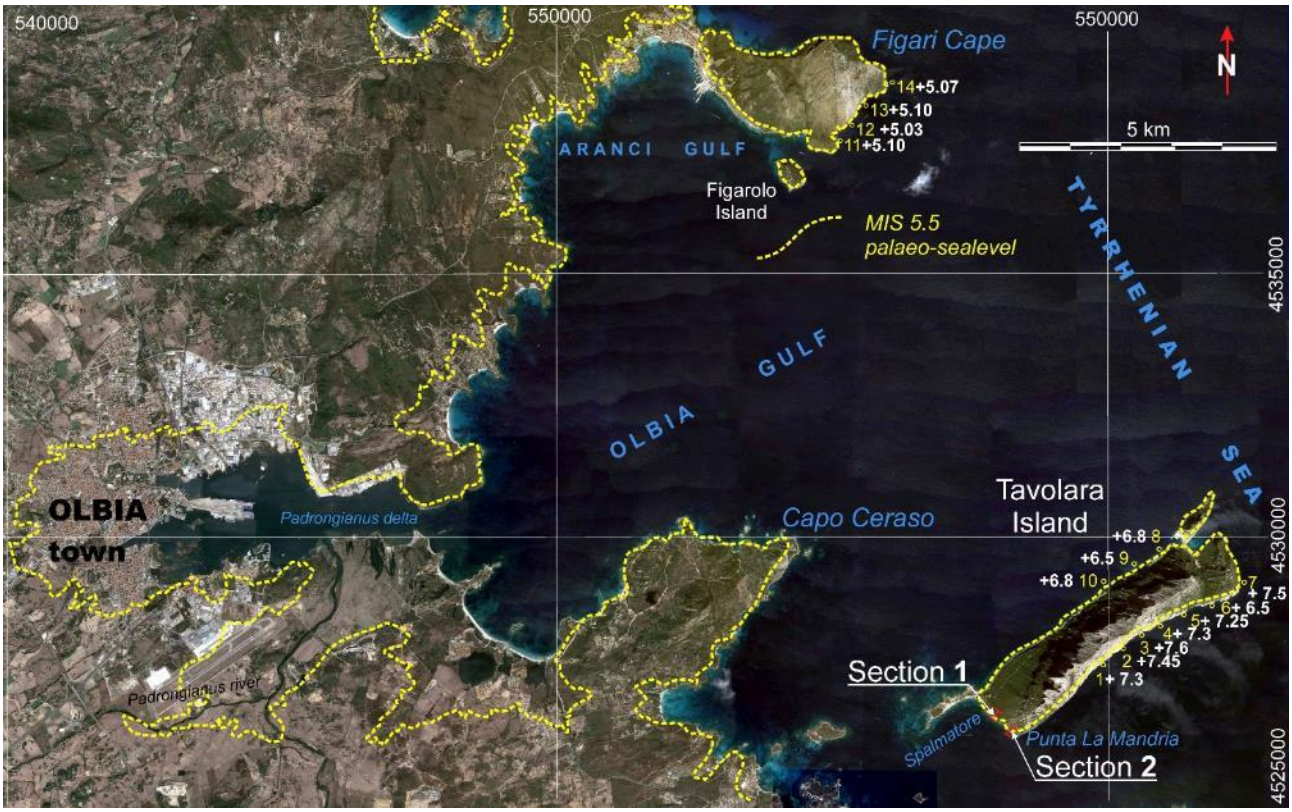

Preprints (www.preprints.org) | NOT PEER-REVIEWED | Posted: 13 August 2021

Figure 9 - Aerial photograph of the coastal plain and the Gulf of Olbia, between the Figari Cape to the north and the Tavolara Island to the south, yellow dashed line indicates the palaeo high sea level of MIS 5.5. Location of MIS5 stratigraphic sections (Fig. 11): **Section1**, on the Tavolara Island, east coast of the bay of Spalmatore. **Section 2**, near the promontory of Punta La Mandria, southernmost point of the Tavolara Island, and and elevations of the tidal notch of the MIS 5.5 [36].

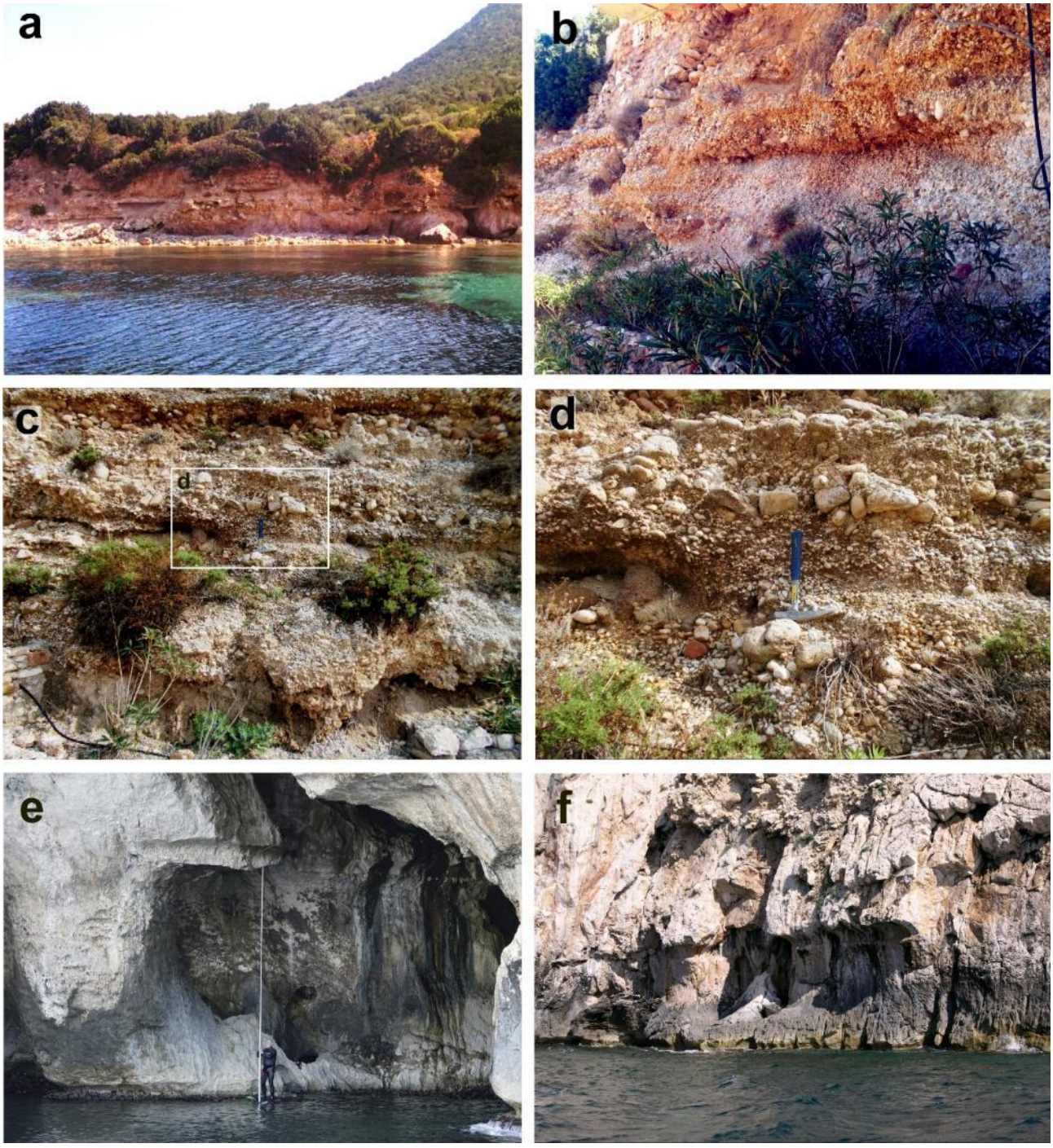

Figure 10 - **a**) a view of the section of Spalmatore Bay marine interglacial fossiliferous sediments transgressive on the granite substrate, **Section 1** [8,35,36]; **b**) conglomeratic heterometric and polygenic fossiliferous level at the bottom weakly cemented sandstones in parallel plane lamination; **c**) Section of Punta La Mandria (**Section 2**) Heterometric conglomerate in an arenaceous matrix with a high fossil content resting on a surface of irregular erosion engraved in the dolomitic limestones of Punta La Mandria;

Preprints (www.preprints.org) | NOT PEER-REVIEWED | Posted: 13 August 2021

d) detail of the previous image, of the conglomerates and microconglomerates containing the remains of gastropods (*Patella ferruginea, Verithium vulgatum; Cipraea lurida*) e lamellibranchi (*Spondilus gaederopus; Mitililus galloprovincialis, Arca noae; Venus verrucosa*). **e**) Tidal notch at + 7.5 m in the north-eastern sector of the Island of Tavolara, Grotta del Papa, altitude measurement through a precision telescopic staff. **f**) Tidal notch (2) at + 7.3 m in the eastern sector of the Island of Tavolara. Part of the continental deposit can be seen at the base, Aeolian sandstones at the base and on the slope at the top that fossilized the MIS 5 palaeo tidal notch.

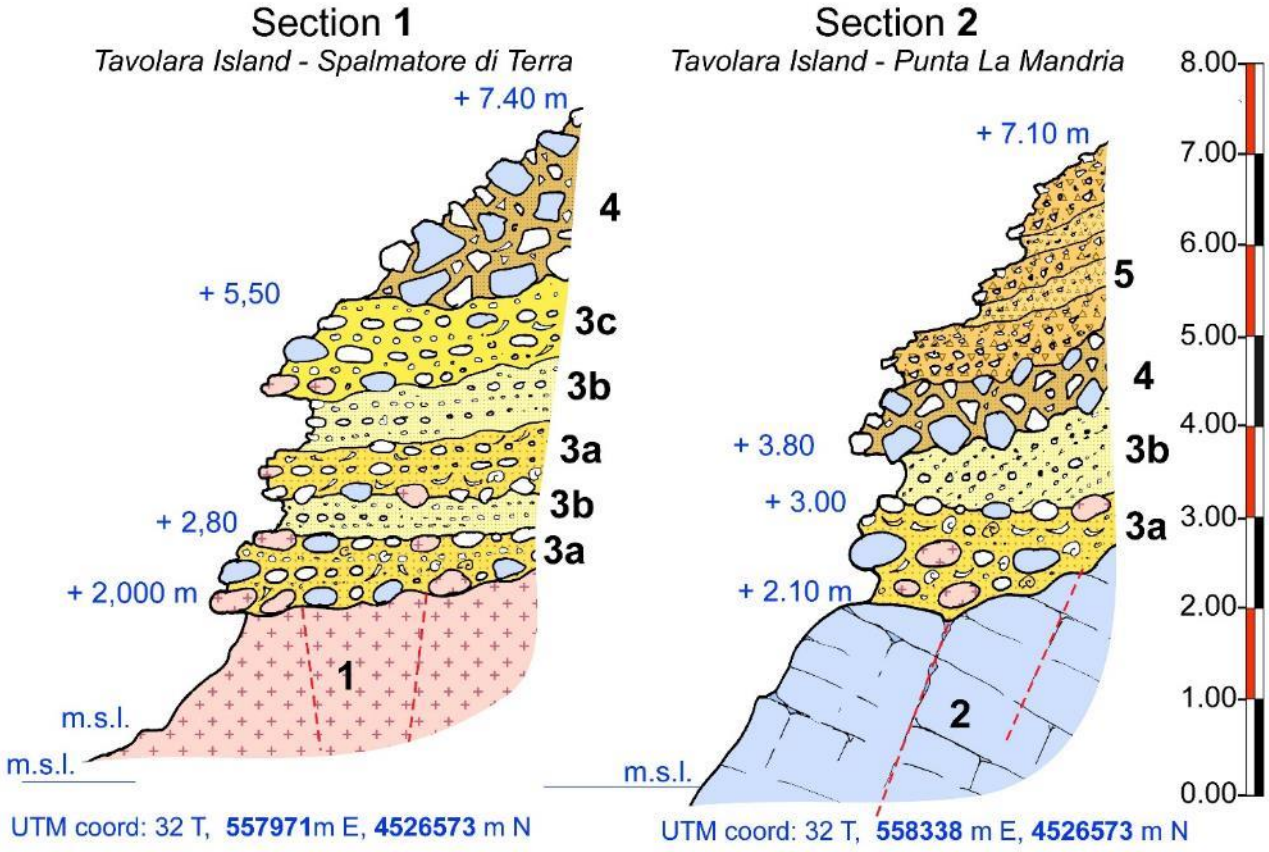

Figure 11 Stratigraphic sections of theMIS 5.5littoral deposits in Tavolara Island, in front of the Olbia coastal plain coastal. **1**) Section of Spalmatore Baya (Sec. 1), inequigranular medium-grained pink leucogranites with phenocrysts of quartz and K Feldspars (Upper Carboniferous). - **2**) Section of Punta La Mandria (Sec. 2), dolomite arenaceous, dolomitic limestone from coasts to circalittoral, with foraminifera and red algae (Dorgali Formation, Middle Jurassic). **3a**) polygenic heterometric conglomerate with with alternating quartz micro-conlomerates in fossiliferous arenaceous matrix (MIS5); **3b**) sandstones and micro-conglomerates mainly quartz, fossiferous with plane-parallel and foreset lamination (MIS5); **3c**) Heterometric conglomerate of granite and dolomite blocks, in an arenaceous matrix with carbonate cement; **4**) Well cemented landslide deposit (MIS 4-3?); **5**) Deposit of stratified slope with alternations of Eboulis ordonnés and Grezes litees (LGM – MIS 2).

3.2 Geomorphology and altitude of MIS 5.5 in Pontina Plain

Located in Italy, south of Rome, the Pontina Plain plain is bordered to the north by volcanoes and pyrso-clastic deposits of Albani hills, to the east by the Lepini and Ausoni mountains (Mesozoic carbonates complexes) and to the west by the Tyrsrhenian sea (Figure 12). This area is characterized by a distensive tectonic regime, that was active during the Pliocene and

Preprints (www.preprints.org) | NOT PEER-REVIEWED | Posted: 13 August 2021

the Quaternary, linked with the tectonic opening of the Tyrsrhenian Sea. In this context, the Piana Pontina represents a sector of particular geological complexity, as the interaction of sea level change with neotectonic phenomena.

Forms and deposits aged MIS 5.5, in particular fossil tidal notches and Cerastoderma living in lagoons, are considered the best markers to detect even small vertical tectonic movements occurred during the last Interglacial [7,8]. As regards the research and studies published for the Quaternary (Upper Pleistocene) of the Pontina Plain, they began in the 1930s and continued until 2018 with study, analysis and dating of new fossil deposits, cores or fossil tidal notches [7,17,37,38,39,40,41,42,43,44,45,46].

We can divide the Pontina Plain into two completely different geomorphological areas: a sandy aeolian portion called Duna Rossa [47] with developed palaeosols that the preserved erosion and morphology which extends from the Tyrrrhenian sea coast up to about half Pontina Plain (with altitudes between 15 up to 30 m) and a silty peaty portion (subject to strong compaction starting from 1930s) with altitudes reaching 5 meters to the north and up to -3 meters to the south near the carbonatic mountains. The negative altitudes are due to: i) extensive subsidence phenomena caused by the drying of peat up to over 6 meters [48]; ii) sinkhole phenomena in the Pontina Plain eastern portion near the contact with Mesozoic carbonates; iii) possible direct fault actions that lower the Mesozoic carbonates under the Pontina Plain (Figure 12). The lower elevation portion of the Plain is towards the eastern portion which is bordered by the Lepini mountains (Mesozoic Carbonates) which, with direct faults, “descend” under the plain; towards the west it borders the formation of the Duna Rossa, aeolian sands aged from to Middle Pleistocene, MIS 5.5, MIS 4, 3 an 2: these deposits are engraved to the north by some reclamation drainage channels including (at Borgo Sabotino) the “Mussolini channel) whose excavation allowed the Persistrombus latus findings [8,46] place them at +10 meters), but after a careful reading of the original paper by [49] we can conclude that the highest deposits of the central\southern Pontina Plain containing Persistrombus latus are located at +5.3 m, the northern portion, near Rome. Blanc, on 1957 performed at Canale Mussolini, one the first radiocarbon age of Europe dating the deposits older of MIS 5.5: wood and peat, attributing them to MIS 4. In the higher levels [50] published an interesting mammalian fauna with Megaloceras, Equus idruntinus, Ursusu speleus. On the depressed peaty area of Pontina Plain (Figure 13) the MIS 5.5 deposits dated with Aminostratigraphy [17] are found between +3 meters to -2 meters. These negative altitudes, often present in the Pontina (up to -4 meters) derive in part from the reclamation that has left up to 16 meters [48] of peat which causes drying produce a considerable subsidence, especially in correspondence with some areas (former sinkholes) close to the limestones of the Lepini-Ausoni mountains.

Preprints (www.preprints.org) | NOT PEER-REVIEWED | Posted: 13 August 2021

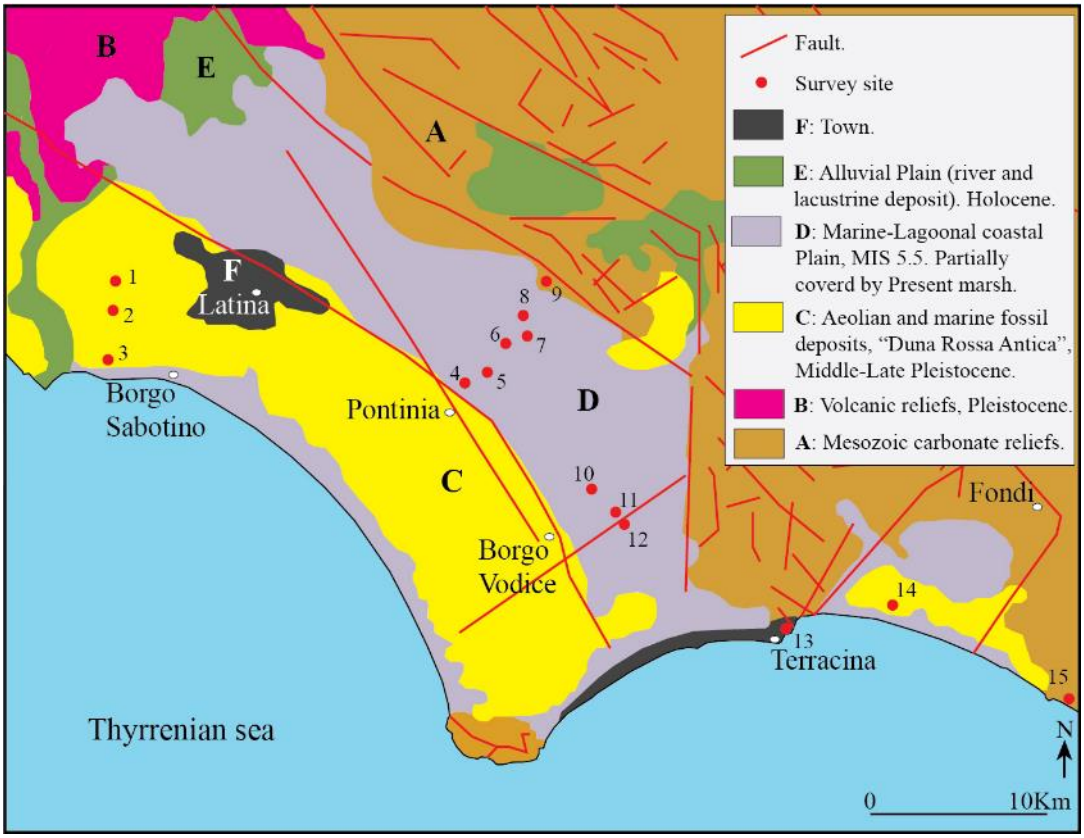

Figure 12. - Main geological outcrocps of the Pontina Plain, this map is a compilation of: i) Italian Geological Survey sheet numbers 170, 158 and 159; ii) Map of the soil [51], iii) sinkhole map of Regione Lazio http://www.regione.lazio.it/binary/rl_main/tbl_documenti/AMB_PBL_Carta_Sinkholes_Lazio_2011.pdf. The red dots refer to the sites described in Table 3.

Preprints (www.preprints.org) | NOT PEER-REVIEWED | Posted: 13 August 2021

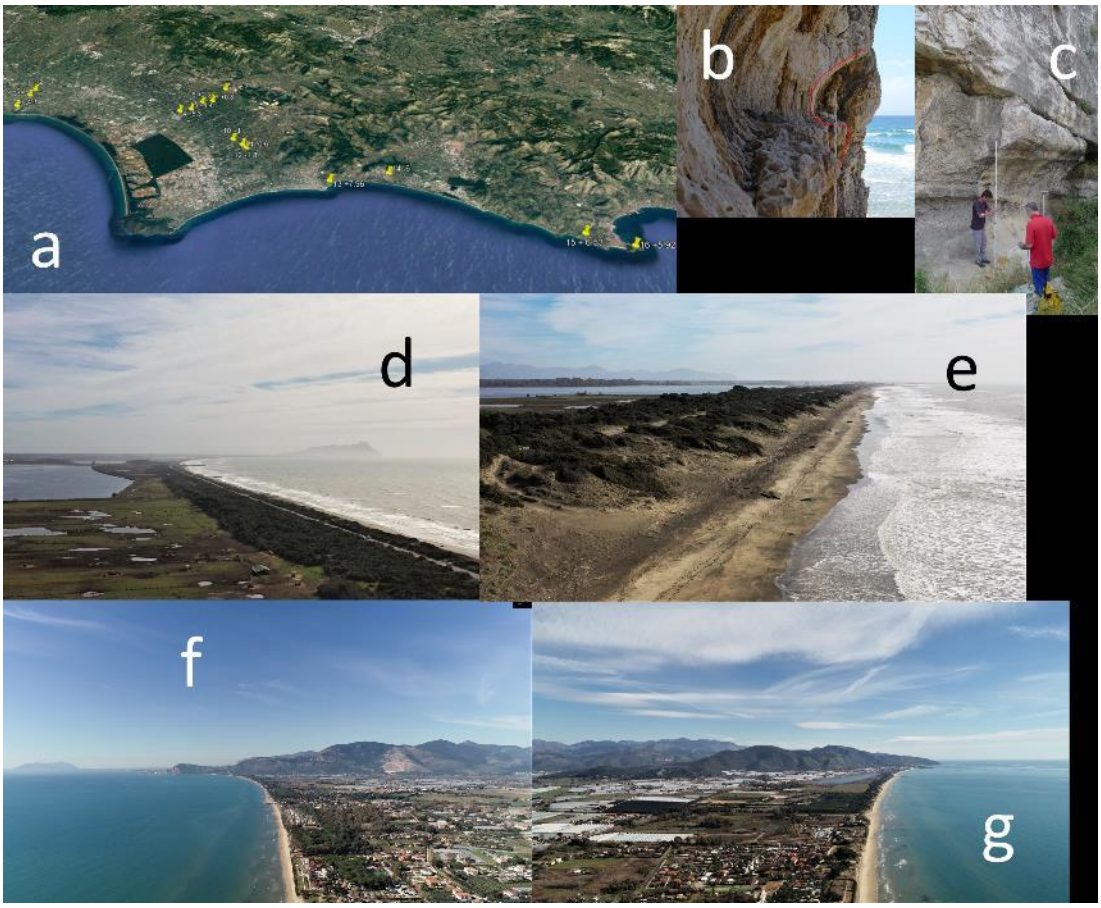

Figure 13. a, Google earth image of the Pontina and Fondi Plain with the carbonatic promontory of Terracina, Sperlonga on which are carved the fossil tidal notches (b and c) aged MIS 5.5 the yellow arrow indicate samples number and altitude (see Table 3) Pianura Pontina e di Fondi. d, the coastal area of northern Pontina Plain (on background he limestone Circeo Promontory); e, the coastal area of northern Pontina Plain (on background he limestone Terracina promontory. f, the coastal area of Fondi Plain (on background the limestone Terracina Promontory; g same point but a southern view, with Sperlonga promontory.

Preprints (www.preprints.org) | NOT PEER-REVIEWED | Posted: 13 August 2021

Figure 14. a: *Cerastoderma edulis* sampled in a section outcropping in the channel of this figure in **e**. **b** *Tapes decussatus* from the outcrop on the reclamation drainage c channel; **c** and **e** the channel d the Mussolini channel during the excavation in 30s; **f** *the outcrop Nassa mutabilis Tapes decussatus*, *Cerastoderma edulis;* **f** a fossiliferous level very rich of lagoon fauna. See also Table 3 site 7.1.

Table 3 On this table all the outcrops dated to MIS 5.5 found studied in the Pontine Plain from Borgo Sabotino (NW) to the Piana di Fondi (SE) and the carbonate promontories of Sperlonga and Gaeta are listed (Figures 13 and 14). In particular, for the lagoon facies sites found in sector D of the of Figure 12 and published in by [17] (Pontinia and Borgo Vodige), an in-field check was carried out with respect to the presence of fossil deposits, their share, and the fossiliferous association. E Images of channels in the silty portion of the Pontina and Fondi Plain. The flow of the springs in conjunction with moments of high tide can lead to the deposition silts that are flooded and some-times partially cover the Mis 5.5 fossil lagoon that extends inland for tens of kilometers.

	A	*B*	*C*	*D*	*E*	*F*
n.	***Site***	**Coordinates**	**MIS 5.5 Altitude (m)**	**Kind of marker**	**Age**	**References**
1	Fosso Moscarello Gnif Gnaf, Santa Maria	41.4615 12.8112	**10 ± 1**	Fossil beach containing *Persistrombus latus*	Senegalese Fauna Aminoacid	[52,53]
2	Canale Mussolini	41.4483 12.8107	**5.1 ± 0.1**	Fossil beach containing *Persistrombus latus*	Senegalese Fauna Aminoacid	[37,40,43]

Preprints (www.preprints.org) | NOT PEER-REVIEWED | Posted: 13 August 2021

3	Nuclear power plant Borgo Sabotino	41.4231 12.8053	**-4.3 +5 ± 0.5**	Fossil beach containing *Persistrombus latus*	Senegalese Fauna	[43]
4	Pontinia 1	41.4129 13.0449	**+5.3 ± 0.5**	Lagoonal facies with *Cerastoderma s.p.*	Geomorphological correlation	[17,46]
5	Pontinia 2	41.4172 13.0600	**+4.4 ± 0.5**	Lagoonal facies with *Cerastoderma*	Geomorphological correlation	[17,46]
6	Pontinia 3	41.4323 13.0721	**+2.3 ± 0.5**	Lagoonal facies with *Cerastoderma s.p.*	Geomorphological correlation	[17,46]
7	Pontinia 4	41.4355 13.0864	**+0.8 ± 0.5**	Lagoonal facies with *Cerastoderma s.p.*	Geomorphological correlation	[17,46]
7.1	Check in field	41.434771 13.062667	**-1± 0.5**	Cerastoderma e Tapes, travertino con incrostazioni	Geomorphological correlation	This paper
7.2	Check in field	41.3757510 13.1281060	**-2± 0.5**	Lagoonal facies with *Cerastoderma s.p.*	Geomorphological correlation	This paper
7.3	Check in field	41.363875 13.140631	**-3± 0.5**	Lagoonal facies with *Cerastoderma edulis, Tapes decussatus, Nassa mutabilis*	Geomorphological correlation	This paper
8	Pontinia 5	41.4424 13.0751	**-0.5 ± 0.5**	Lagoonal facies with Cerastoderma	Geomorphological correlation	[17,46]
9	Mezzaluna core	41 27 47 13 06 01	**-14.30 -11.41 ± 0.5**	Venus and Cerastoderma	Pollen Analysis, U\Th and aminoacid	[45]
10	Borgo Vodige 1	41.3571 13.1317	**1 ± 0.5**	Lagoonal facies with Cerastoderma	Aminoacid	[17,46]
11	Borgo Vodige 2	41.3497 13.1293	**-0.6 ± 0.5**	Lagoonal facies with Cerastoderma	Aminoacid	[17,46]
12	Borgo Vodige 3	41.350 13.117	**-1.80 ± 0.5**	Lagoonal facies with Cerastoderma	Aminoacid	[17,46]
13	Terracina	41.288 13.260	**7.96 ± 0.1**	Tidal notch	Geomorphological correlation at 5 km from aged MIS 5.5 deposit	[7]
14	Fondi APT4	41.0065 13.331	**-6 \ -24**	Marsh with Cerastoderma Aminozone E	Aminoacid	[44]
15	Sperlonga	41.229691 13.502001	**7.30 ± 0.5**		Geomorphological correlation	[8]

Preprints (www.preprints.org) | NOT PEER-REVIEWED | Posted: 13 August 2021

16	Sperlonga	41.2187 13.5321	**6.53 ± 0.1**	Tidal notch	Geomorphological correlation	[44]
17	Gaeta	41.2046 13.5774	**5.92 ± 0.1**	Tidal notch	Geomorphological correlation	[44]

3.3 Maps of the Pontina Plain

On the basis of the maximum altitude of the higstand reached during the MIS 5.5 of 8.2 m, [44] and the Present altitude of the Pontina Plain maps (Table 1), it was possible to reconstruct the transgressive event that occurred 119 ka BP. A gulf that forwards in NW direction for about 32 kilometers, with a total flooded area of 401.42 km^2 (Table 4) and about 100 km of coastline involved in the transgression of 119 ka BP (Table 2). This high sea stationing event is demonstrated by the data (forms and deposits) emerging in the plain and described in the previous chaptera. Based on IPCC 2019 data, in 2300 the maximum elevation of the sea will be 5,249 meters higher than 2019, based on the elevation of the Pontina Plain maps it was possible to reconstruct the possible future transgressive event (Figure 15) Provided that "man" does not carry out any anthropic built (dams, genic interventions (dams, water pumps, ecc. ecc.). Figure 15 show a gulf that will extend into the Piana Pontina for about 26 km and that could have a total flooded area of 306.67 km^2.

Preprints (www.preprints.org) | NOT PEER-REVIEWED | Posted: 13 August 2021

Table 4 A Coastal sites; B Exposure; C Maximum fetch; D **Max fetch**; E **Coastal material**; F **Wave energy Flux kW\m** This is an average between 2 types of data in [54]. Maximum waves and energy are found between the Balearic Islands and Capo Caccia with values between 9 and 10.0.; G **Geomorphology**; H **Flooded area during MIS 5.5 km²**; I projection **Flooded area Ipcc 2300, km²**; L projection **Flooded area IPCC 2100 km²** as regards the flooded area of the Pontina Plain on the map (Figure 13) we divided in 3 different area (Pontina 190 , Fondi 64,5 and Laghi Costieri 49,2; M **Exposed coastline Lenght km**; N **Human-Made Structures**.

A	B	C	D	E	F	G	H	I	L	M	N
Site n°	**Coastal site**	**Exposure direction**	**Max fetch Km**	**Coastal material**	**Wave energy Flux kW\m**	**Geomorphology**	**Flooded area MIS 5.5 km²**	**Flooded area Ipcc 2300 km²**	**Flooded area IPCC 2100 km²**	**Exposed coastline Lenght km**	**Human-Made Structures**
1	Pontina Plain*	N - W	308	sand	3-4	Embayed Beach	396,3	303,7	*61*	104,9	Towns and Agricoultural crops
2	Cagliari	S	208	sand	4-5	Barrier and lagoon systems	131,5	87,2	27,5	29,6	Towns and Agricoultural crops
3	Oristano	W	357	sand	6-7	Barrier and lagoon systems	376,8	230,0	53,5	102,7	Towns and Agricoultural crops
4	Olbia	E	231	sand	3-4	Rias + Barrier and lagoon systems	24,7	16,3	4,53	30,7	Towns, harbor and industrial hub

Preprints (www.preprints.org) | NOT PEER-REVIEWED | Posted: 13 August 2021

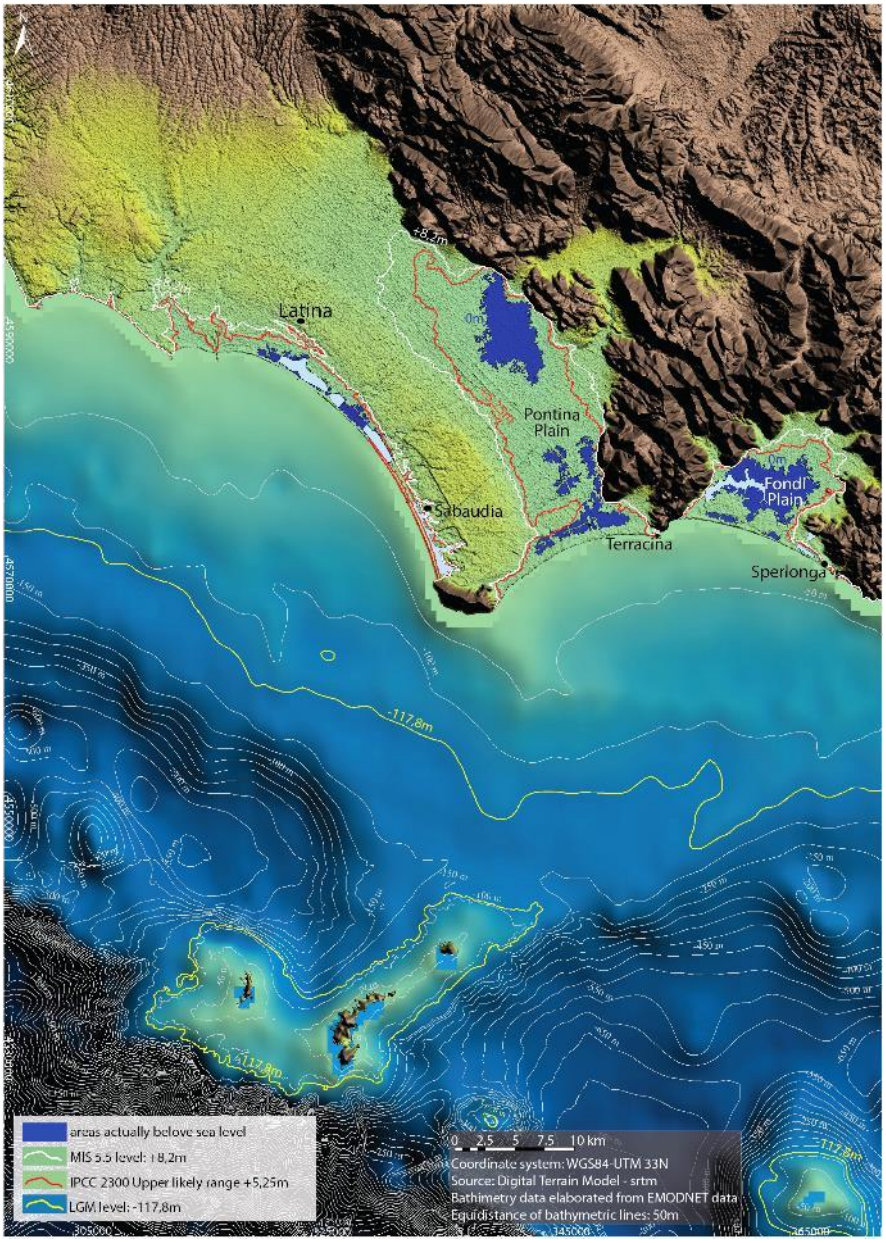

Figure 15 The Pontina and Fondi Plains maps showing the potential submersion area using IPCC AR5 RCP 8.5 for 2100 and 2300: The MIS 5.5 extension occurred 119 ka BP.

3.4 Maps of Cagliari Plain

The northern sector of the Gulf of Cagliari is characterized by a flood plain with a low slope towards South. In this sector, during MIS 5.5, the maximum altitude of +8.4 m above current sea level originated two bays: one to the west (current Laguna di Santa Gilla) with a retreat of the shore line of about 16 km and one to the east (current Molentargius) with a retreat of about 6 Km. The Sant'Elia promontory was isolated from the mainland and represented an island or was probably connected to the coast through a tombolo. The map shows that in MIS 5.5, the marine transgression affected the coastal sector wide 27 km with a flooded area of 131.54 km^2. The same map shows the maximum level of + 5.25 m compared to the sea level for the year 2300 based on IPCC 2019 data; in particular, the map shows a scenario which about 87.24 Km^2 of coastline are submerged; the sea level rise would lead to the demolition of the Holocene

Preprints (www.preprints.org) | NOT PEER-REVIEWED | Posted: 13 August 2021

littoral spits with a shoreline retreat of 16 km and 14 km, respectively for the Santa Gilla and Molentargius lagoons and the subsequent formation of bay beaches (Figures 16,17)

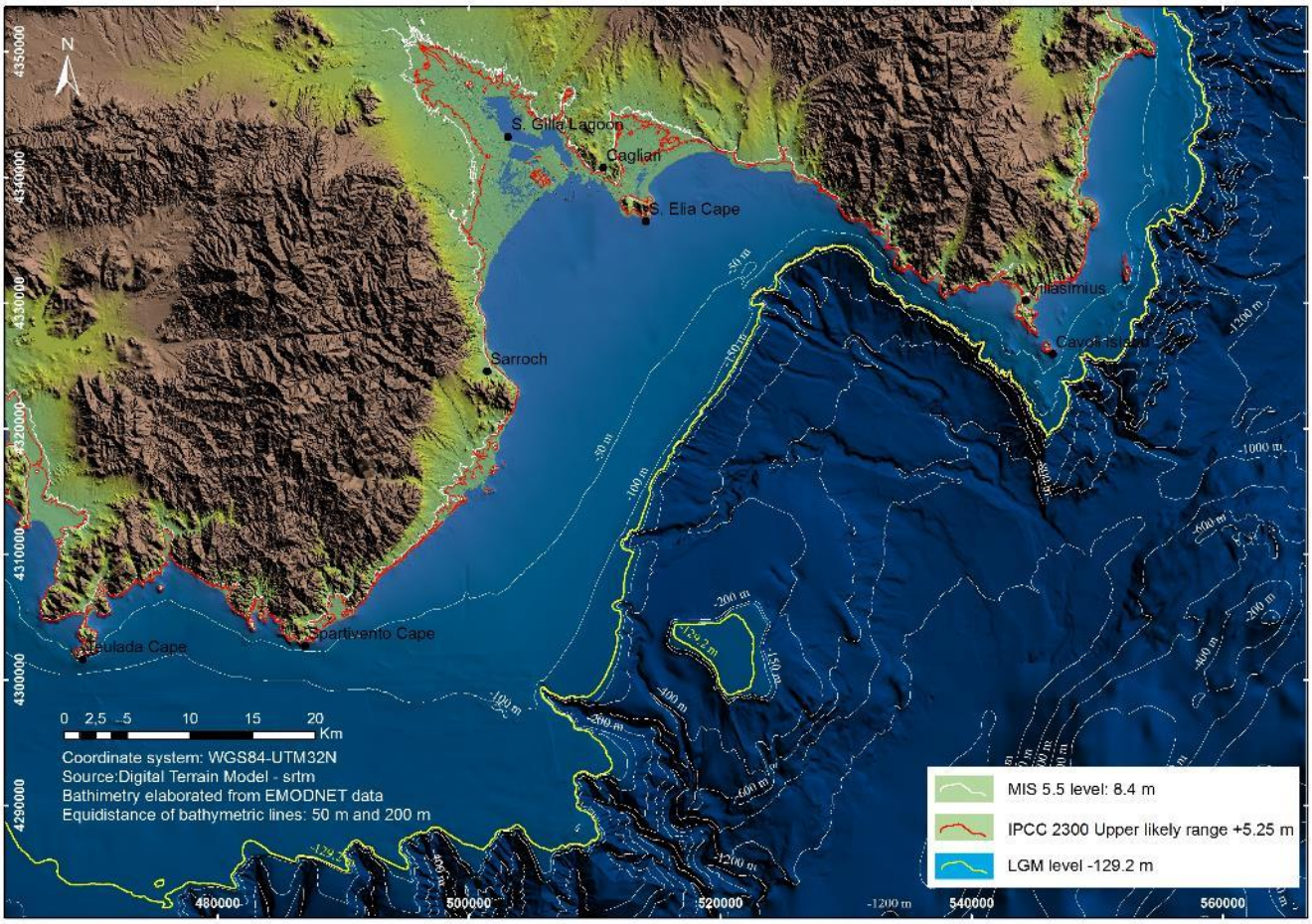

Figure 16 The Cagliari plane map showing the potential submersion area using IPCC AR5 RCP 8.5 for 2100 and 2300: The MIS 5.5 extension occurred 119 ka BP.

Preprints (www.preprints.org) | NOT PEER-REVIEWED | Posted: 13 August 2021

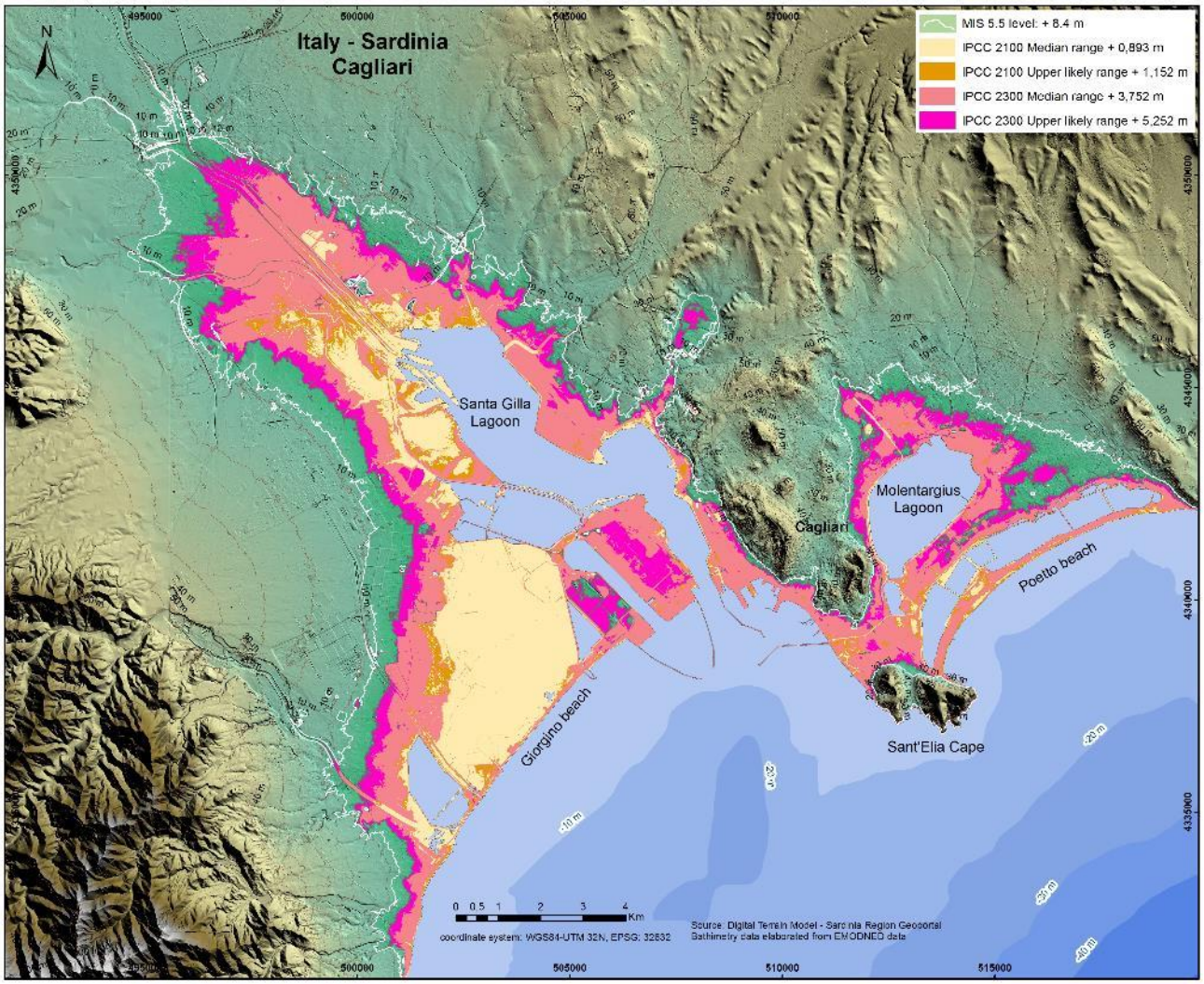

Figure 17 Map of Cagliari plane, (see also Figure 1 for location). The potential submersion area, using IPCC AR5 RCP 8.5 projections at 2100 and 2300.

3.5 Maps of Oristano Plain

In the Gulf of Oristano, the MIS 5.5 shoreline reaches a maximum level of +8.5 m a.s.l.. Also for this sector the slope is very low; there is a maximum shore line retreat about 13 km and the submersion area of about 376.77 km2. The map shows the maximum level of +5.25 m above sea level for the year 2300 based on IPCC 2019 data. This scenario would lead the demolition of the Cabras and Santa Giusta littoral spits, the submersion of 230 km2 in a sector of coastline that extends for 103 linear km and the retreat of the Tirso River mouth towards the north-east (Figure 18, 19).

Preprints (www.preprints.org) | NOT PEER-REVIEWED | Posted: 13 August 2021

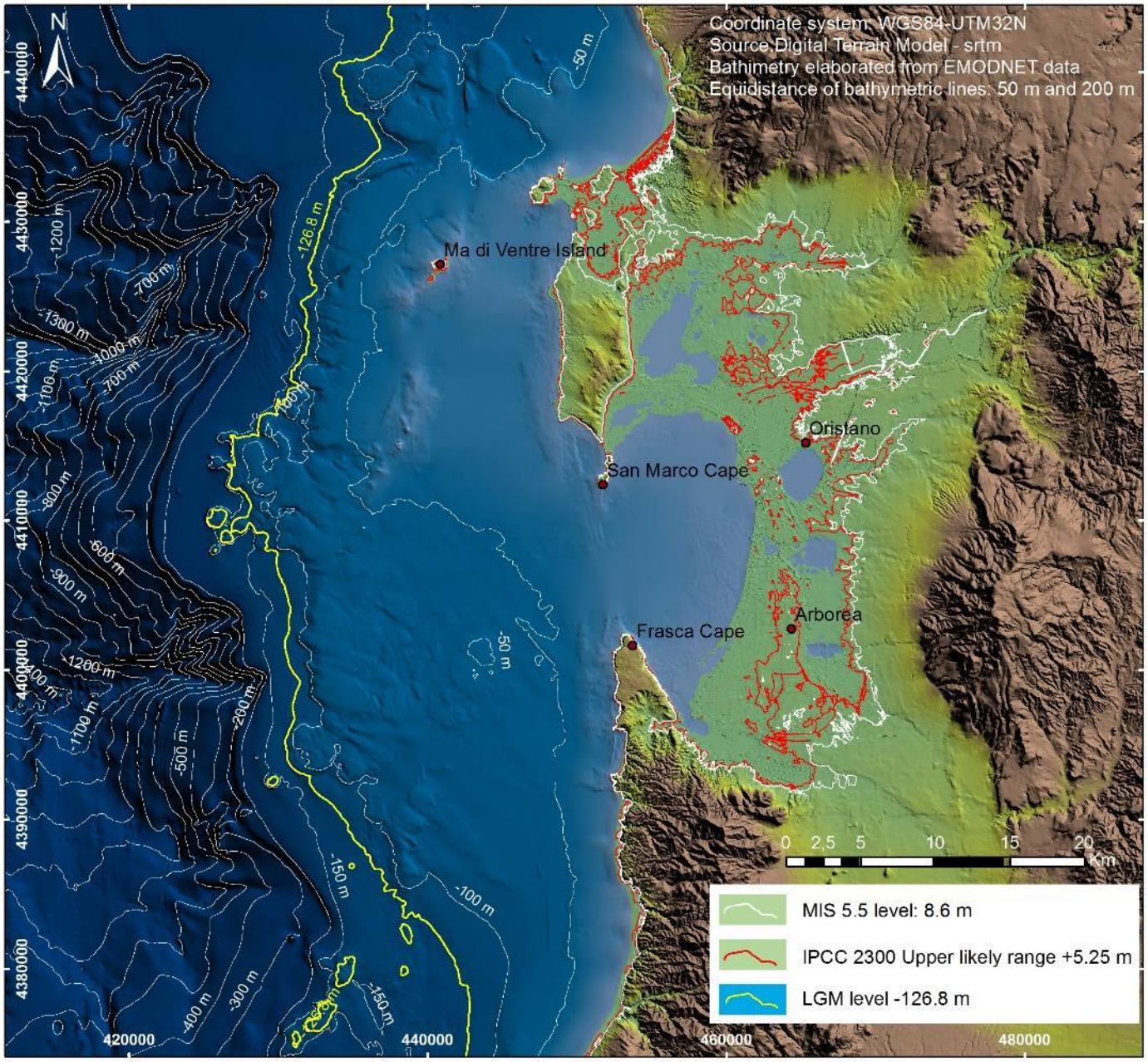

Figure 18 The Oristano plane map showing the potential submersion area using IPCC AR5 RCP 8.5 for 2100 and 2300: The MIS 5.5 extension occurred 119 ka BP.

Preprints (www.preprints.org) | NOT PEER-REVIEWED | Posted: 13 August 2021

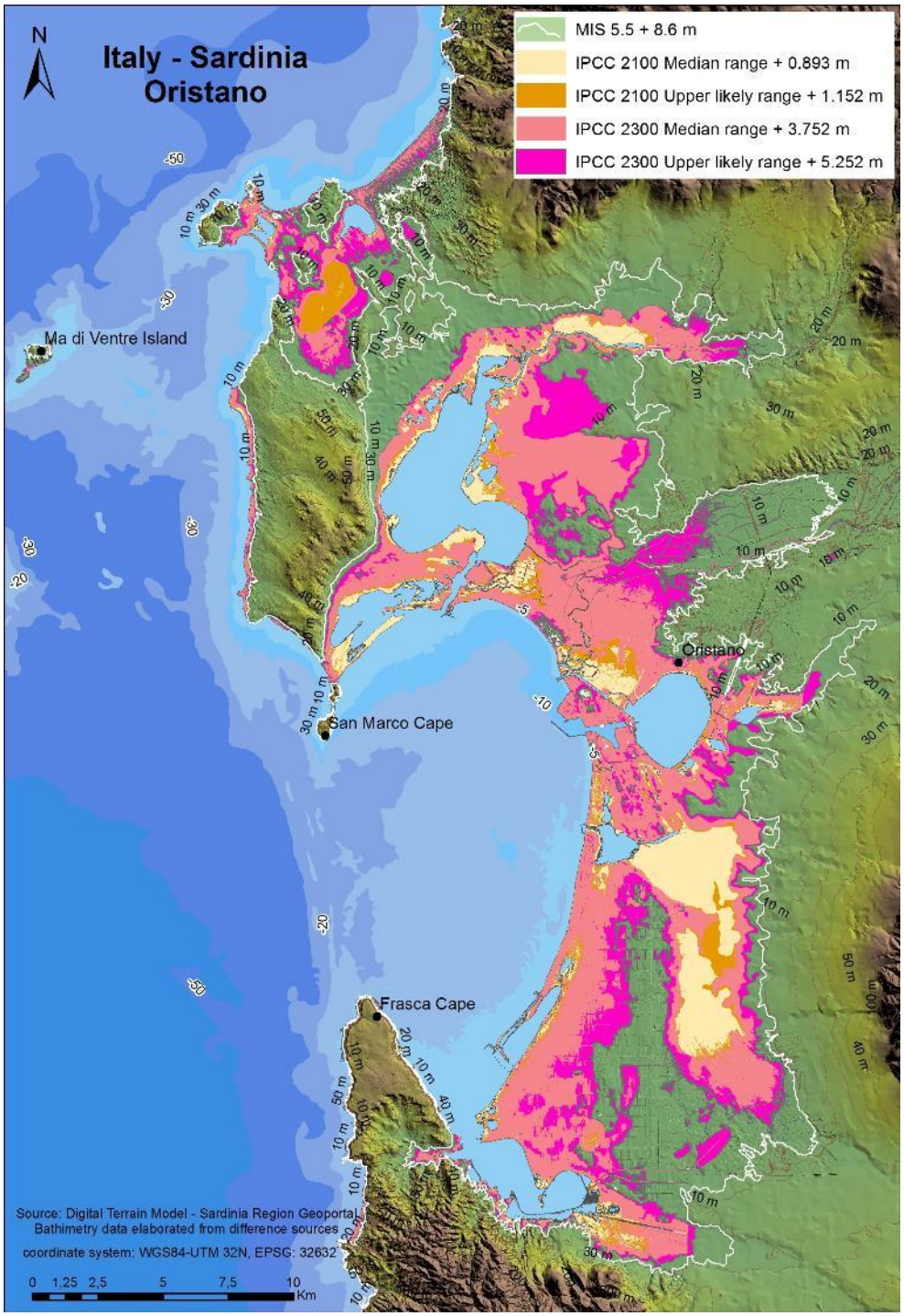

Figure 19 - Map of Oristano plane, (see also Figure 1 for location). The potential submersion area, using IPCC AR5 RCP 8.5 projections at 2100 and 2300.

3.6 Maps of Olbia Plain

The Gulf of Olbia is represented by a rias coast engraved on granite lithologies. The slopes are greater than the alluvial plains of Cagliari and Oristano. For this reason, the MIS 5.5 sea level with an altitude of + 8.5 m a.s.l. it is measured up to a maximum of 2 km from the current shoreline while the submerged surface during MIS 5.5 was equal to 24.69 km2. For this area, the sea level on the basis of IPCC 2019 data will reach the maximum altitude of + 5.25 with the submersion of 16.31 Km2 of coastal area. The map shows the demolition of the lagoon behind

Preprints (www.preprints.org) | NOT PEER-REVIEWED | Posted: 13 August 2021

Le Saline beach, the retreat of the Rio Padrongianus mouth and the retreat of approximately 1 km in correspondence of the City of Olbia (Figures 20,21).

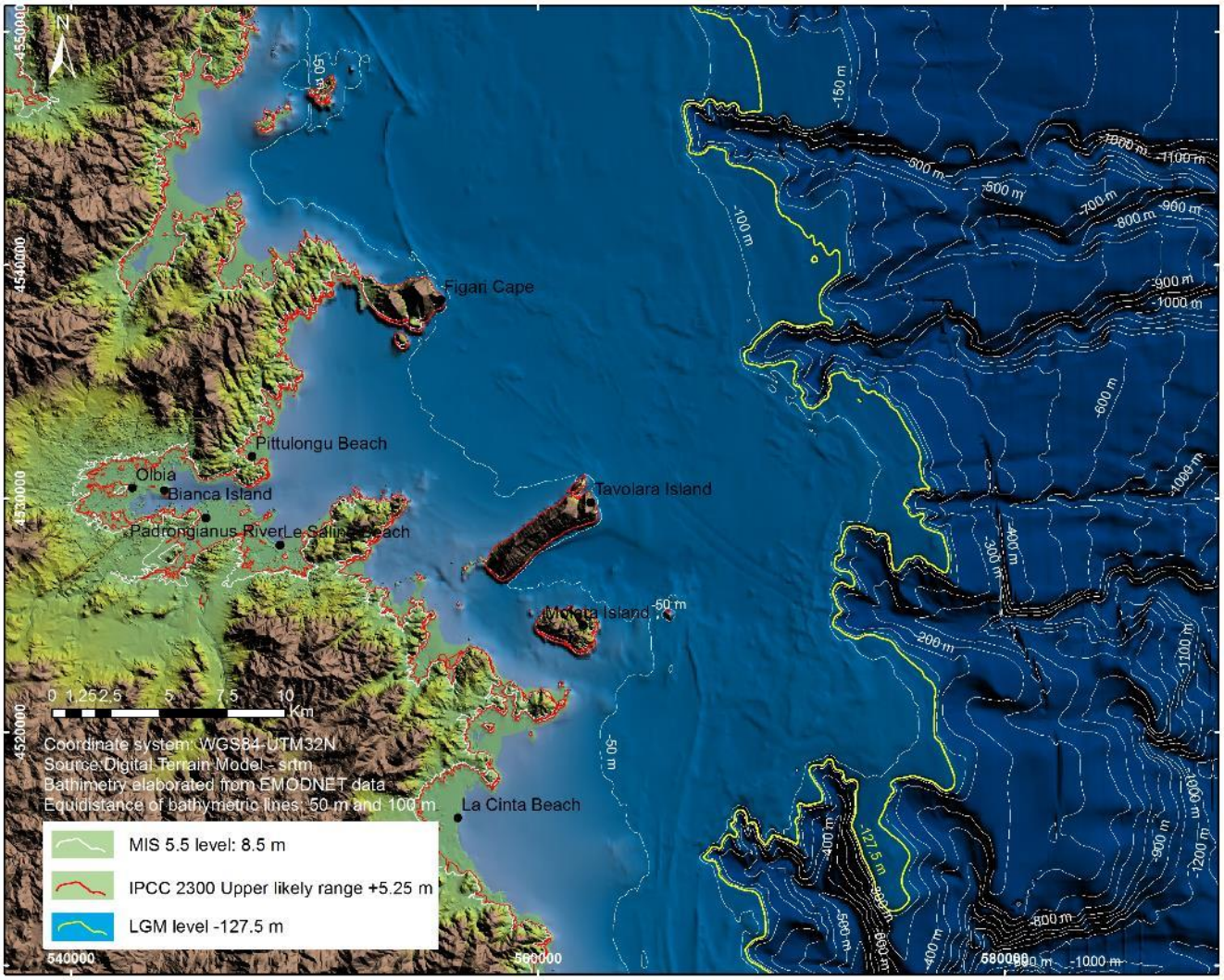

Figure 20 Olbia plane map showing the potential submersion area using IPCC AR5 RCP 8.5 for 2100 and 2300: The MIS 5.5 extension occurred 119 ka BP.

4. Discussion

The palaeoclimatic events that 125.000 yrs BP have led to a notable ice melting with a global consequence of a sea level rise more than 5-7 meters around the world, are still the subject of scientific debate. As regard the CO2 content in the atmosphere, 119 ka BP, was considerably lower than today, but the insolation was higher. In fact, such a high sea level (and carbon dioxide in the atmosphere) was never reached except in the Pliocene [55,56]. Gilford et al 2020 [57] explores the extent to which MIS 5.5 constraints could inform future Antarctic contributions to sea-level rise, forcing Last Interglacial with IPCC RCP8.5, obtaining a sea level over year 2150 of about 5 meters even beyond the 2019 IPCC forecasts.

As regards data and interpretations on insolation due to astronomical variables dynamics of are not univocal, and are difficult to compare with each other due to the different measurement methods and sensors [58,59]. Datasets of daily SSR records (1953-2013) were interpolated on a regular grid and grouped into two regions, northern and southern Italy, both in all-sky and clear-sky SSR mode. [60].

Preprints (www.preprints.org) | NOT PEER-REVIEWED | Posted: 13 August 2021

While taking into account the IPCC literature which mainly indicates a phase of decrease in insolation in the last 6 ka while the warming recorded in the last 2 centuries is due to the increase in CO2 (IPCC 2019).

The possibility is also considered that, on the contrary, there is an increase in the insolation of astronomical origin (Milankovic cycles) characteristic of an Interglacial phase [61,62], a condition that finds support in the data from geo-archaeological indicators of the last 4 Ka [32]. In this case, the increase in CO2 would contribute to global warming by accelerating the upward trend of the sea level. [2].

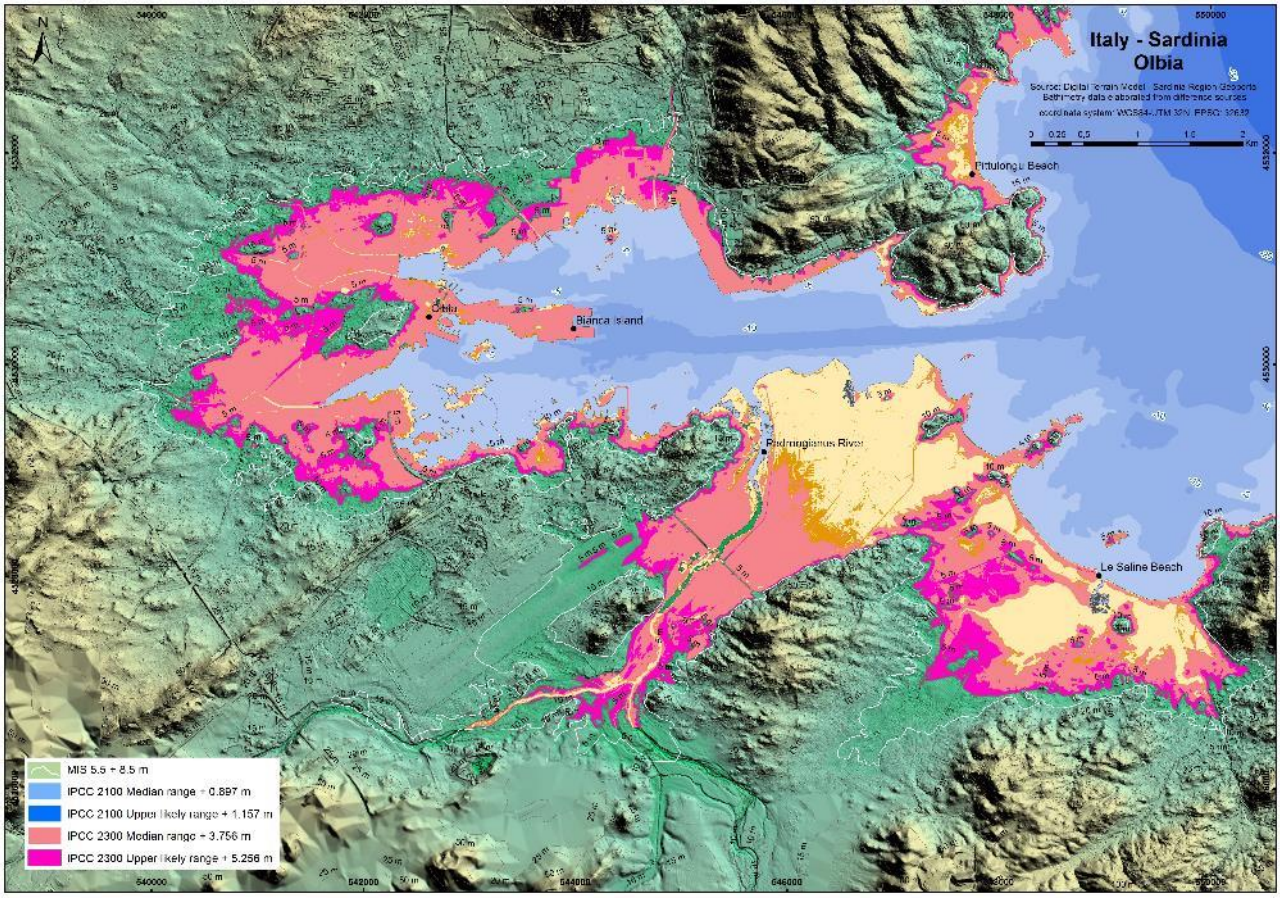

Figure 21 Map of Olbia plane, (see also Figure 1 for location). The potential submersion area, using IPCC projections at 2100 and 2300**.**

For all these reasons we think that the approach of using the maximum transgression occurred 119 ka BP has serious scientific motivations. None of the Authors are hoping for a sea level rise above 1 meter in 2100, but at the light of what happened during MIS 5.5 it seemed useful to have a realistic view of the effects. The maximum altitude that sea level reached during MIS 5.5 can therefore be considered as a reference also for there future sea level rise.

4.1 Pontina Plain

The Pontina Plain map (Figure 15) highlights a deep palaeogulf that falls for 33 km. It should also be emphasized that the eastern portion of the Pontine plain is subject to a subsidence partly induced by the reclamation, partial drying of the peat and partly to negative tectonic movements, especially in correspondence with the eastern edge of the Pontine plain in contact with the Mesozoic carbonate. In some areas of the Pontine Plain we find lagoonal deposits containing Cerastoderma edulis outcropping in field down to -2 meters, these

Preprints (www.preprints.org) | NOT PEER-REVIEWED | Posted: 13 August 2021

circumstances confirm small but continuous negative vertical movements especially in the southern portion of the Plain (Figure 15).

4.2 Sardinia

4.2.1 Cagliari coastal plain

The map of the Cagliari Coastal Plain highlights 2 deep inlets separated by the high structural system of Cagliari Hills - Cala Mosca-Sella del Diavolo Promontory. The eastern inlet gave rise to the Molentarigius paleo-lagoon, closed by the littoral spit of Is Arenas (Fig. 3; Fig. 5 - Section 3). In the sector of maximum expansion of the Last Interglacial transgression, strips of the inner margins engraved in MIS 6 alluvial deposits are preserved (Fig. 5 - Section4).

The western bay deepens into the plain for about 15 km. The MIS 5.5 transgression internal margin present a marine terrace at Cerastoderma glaucum [24] which a strip was found at +3.40 m (Fig. 5 - Section 5). The coastal palaeo-spit marine deposits of Sa Illetta, which closed the palaeo-lagoon of Santa Gilla, were found up to an altitude of + 4.30 m, while in correspondence of the 2 lagoon palaeo-mouths of the the MIS 5 fossiliferous levels are found at - 2 m (east lagoon-mouth) and - 5 m (west lagoon-mouth - La Plaja coastal spit).

4.2.2 Oristano-Sinis coastal plain

In the sector of Oristano-Sinis the Last Interglacial transgression enters in the coastal plain of Cabras for about 10 km, no inner margin was clearly detected as it is covered by river and slope deposits. A paleo-spit closes the paleo-lagoon of Cabras (fig. 6) with littoral sediments detected up to an altitude of 4.30 m (Fig. 8 - Section 2).

The maximum altitude of the littoral deposits of MIS 5 was found in San Giovanni di Sinis where sandstone with pianopalallel lamination reaches + 5.50 m (Fig. 8 - Section 1), while on the eastern coast of the di Capo San Marco promontory an abrasion platform engraved in the Pliocene basalts with an inner margin at an altitude of + 7 m is present.

4.2.3 Olbia coastal plain and Tavolara Island

The littoral deposits of the Olbia coastal plain were extensively studied by Aldo Segre in 1954, the significant increase in tourist construction on the coast during about 70 years has obliterated most of the outcrops that have instead been preserved on the Tavolara island (for decades National Marine Protected Area). (Fig. 9)

The upper limit of the Last Interglacial is well marked in the area with by tidal noches, at + 7.5 m at Grotta del Papa (Fig. 11 - e)

The MIS 5 fossiliferous deposits of Spalmatore di Terra (Tavolara Island), in high energy facies (conglomerates and microconglomerates) reach + 5.5 m (Fig. 11- Section 1).

Fossil deposits similar to those of MIS 3 were crossed by geotechnical cores at an altitude of - 4 m in the area of the Inner Port of Olbia, a port area located in the bottom of the bay set on a deep Ria with a tectonic setting.

5. Conclusions

In this work, we have shown a methodology to create precise maps with a potentially expected submersion scenarios for 2100 in 4 selected coastal zones of the Mediterranean basin which are prone to marine submersion under the effects of relative sea-level rise. For these areas,

Preprints (www.preprints.org) | NOT PEER-REVIEWED | Posted: 13 August 2021

were produced thematic maps that were based on climatic scenarios, tectonics, local geological behavior and the best available digital topography.

Some areas guest natural high value sites belonging to protected areas or National Parks; some are deeply urbanized by residential or touristic settlements; others are characterized by the presence of cultural heritage, and infrastructure such as communication routes and harbors.

From our analysis we estimated that during MIS 5.5 for the whole studied sites was flooded by the sea an area of 929,3 Km2. 396, 3 Km2 in the Pontina Plain, 131, 5 Km2 in the Cagliari Plain, 376,8 for Oristano Plain and 24,7 for Olbia Plain. Potential loss of land for the above areas at 2300 of 146,5 Km2, at 2100 of 146,5 Km2 for the IPCC-RCP8.5 whole sites studied, impacting a coastline length of about 267,9 km. In these coastal areas are often located densely inhabited settlements and infrastructures. The expected scenario and the exposition of the investigated areas to coastal hazard should be considered for a cognizant management of the coastal zone.

The comparison between the maximum ingression line of the Last Interglacial and the present evolutionary trend of submersion of the coastal plains is justified by the fact that, at the current state of knowledge, it cannot be excluded that maximum altitude that sea level reached during MIS 5.5 can therefore be considered as a reference also for the future sea level rise.

Supplementary Materials: The following are available online at www.mdpi.com/xxx/s1, Figure S1: title, Table S1: title, Video S1: title.

Author Contributions: For research articles with several authors, a short paragraph specifying their individual contributions must be provided. The following statements should be used "Conceptualization, G.D., F.A., P.O and V.L.; methodology, G.D., F.A. and V.L; software, G.D., L.M. and V.L.; validation, F.A. and P.O.; formal analysis, G.D., F.A., P.O and V.L; investigation, G.D., F.A., P.O and V.L.; resources, G.D., F.A., P.O and V.L.; data curation G.D., G.R. and V.L.; writing—original draft preparation, G.D. and V.L.; writing—review and editing, G.D., F.A., P.O and V.L.; visualization, G.R.; supervision, F.A. and P.O.; project administration, G.D., F.A., P.O and V.L.; funding acquisition, F.A. and P.O. All authors have read and agreed to the published version of the manuscript.".

Funding: This research received no external funding

Data Availability Statement:

Acknowledgments: In this section, you can acknowledge any support given which is not covered by the author contribution or funding sections. This may include administrative and technical support, or donations in kind (e.g., materials used for experiments).

Conflicts of Interest: "The authors declare no conflict of interest

References

1. H.O. Pörtner, D.C. Roberts, V. Masson-Delmotte, P. Zhai, M. Tignor, E. Poloczanska, K. Mintenbeck, M. Nicolai, A. Okem, J. Petzold, B. Rama, N. Weyer (eds.). Cambridge University Press, Cambridge, United Kingdom and New York, NY, USA, **2019**. IPCC, 2019. *Special Report on the Ocean and Cryosphere in a Changing Climate*. https://www.ipcc.ch/srocc/home/
2. Vacchi M, Joyse KM, Kopp RE, Marriner N, Kaniewski D & Rovere A. Climate pacing of millennial sea-level change variability in the central and western Mediterranean. Nature Communications. **2021**, 12, 4013. https://doi.org/10.1038/s41467-021-24250-
3. Lambeck, K.; Antonioli, F.; Anzidei, M.; Ferranti, L.; Leoni, G.; Scicchitano, G.; Silenzi, S. Sea level change along the Italian coast during the Holocene and projections for the future. *Quat. Int.* **2011**, *232*, 250–257, doi:10.1016/j.quaint.2010.04.026.
4. Antonioli, F.; Anzidei, M.; Amorosi, A.; Lo Presti, V.; Mastronuzzi, G.; Deiana, G.; De Falco, G.; Fontana, A.; Fontolan, G.; Lisco, S.; et al. Sea-level rise and potential drowning of the Italian coastal plains: Flooding risk scenarios for 2100. *Quaternary Science Reviews* **2017**, 158, 29–43, doi:10.1016/j.quascirev.2016.12.021.
5. Marsico, A.; Lisco, S.; Presti, V.L.; Antonioli, F.; Amorosi, A.; Anzidei, M.; Deiana, G.; Falco, G.D.; Fontana, A.; Fontolan, G.; et al. Flooding scenario for four Italian coastal plains using three relative sea level rise models. Journal of Maps, **2017**, 13, 961–967, doi:10.1080/17445647.2017.1415989.

Preprints (www.preprints.org) | NOT PEER-REVIEWED | Posted: 13 August 2021

6. Bonaldo, D.; Antonioli, F.; Archetti, R.; Bezzi, A.; Correggiari, A.; Davolio, S.; De Falco, G.; Fantini, M.; Fontolan, G.; Furlani, S.; et al. Integrating multidisciplinary instruments for assessing coastal vulnerability to erosion and sea level rise: lessons and challenges from the Adriatic Sea, Italy. J Coast Conserv **2019**, 23, 19–37, doi:10.1007/s11852-018-0633-x.
7. Antonioli, F.; Ferranti, L.; Stocchi, P.; Deiana, G.; Lo Presti, V.; Furlani, S.; Marino, C.; Orru, P.; Scicchitano, G.; Trainito, E.; et al. Morphometry and elevation of the last interglacial tidal notches in tectonically stable coasts of the Mediterranean Sea. *Earth-Science Reviews*, **2018**, 185, 600–623, doi:10.1016/j.earscirev.2018.06.017.
8. Ferranti, L.; Antonioli, F.; Mauz, B.; Amorosi, A.; Dai Pra, G.; Mastronuzzi, G.; Monaco, C.; Orrù, P.; Pappalardo, M.; Radtke, U.; et al. Markers of the last interglacial sea-level high stand along the coast of Italy: Tectonic implications. *Quat. Int.* **2006**, *145–146*, 30–54, doi:10.1016/j.quaint.2005.07.009.
9. Rovere, A. ; Raymo, M. E.; Vacchi, M.; Lorscheid, T.; Stocchi, P.; Gomez-Pujol, L.; Harris, D.L.; Casella, E.; O'Leary, M. J.; Hearty, P. J. The analysis of Last Interglacial (MIS 5e) relative sea-level indicators: Reconstructing sea-level in a warmer world. *Earth Sci. Rev*. **2016**, 159, 404-427, 10.1016/j.earscirev.2016.06.006
10. Berger A.; Loutre M.F. An exceptionally long interglacial ahead? *Science* 2002,297 (5585), 1287-1288 10.1126/science.1076120.
11. Berger, A.; Loutre, M.–F.; Modeling the Climate Response to Astronomical and CO2 Forcings. *Geophys. Extern., Climat et Envir., C. R. Acad. Sci. Paris.* **1996**, 323 (IIa) 1.
12. Loutre, M.F.; Berger, A.; Future Climatic Changes: Are We Entering an Exceptionally Long Interglacial?. *Climatic Change.* **2000**. 46, 61–90. https://doi.org/10.1023/A:1005559827189
13. Berger, A. L. Long-term variations of daily insolation and Quaternary climatic change. *J. Atmos. Sci*. **1978**,35, 2362–2367.
14. Antonioli F., De Falco G., Lo Presti V., Moretti L., Scardino G., Anzidei M., Bonaldo D., Carniel S., Leoni G., Furlani S., Antonella Marsico A.,Petitta M., Randazzo G., Scicchitano, G., Mastronuzzi G.. Relative Sea-Level Rise and Potential Submersion Risk for 2100 on 16 Coastal Plains of the Mediterranean Sea. Water. **2020.**12(8), 2173. https://www.mdpi.com/2073-4441/12/8/2173
15. Ferranti, L.; Antonioli, F.; Monaco, C.; Scicchitano, G.; Spampinato, C.R. Uplifted Late Holocene Shorelines along the Coasts of the Calabrian Arc: Geodynamic and Seismotectonic Implications. IJG. 2017, 136, **2017**, f.3, doi:10.3301/IJG.2017.13.
16. Ferranti, L.; Antonioli, F.; Anzidei, M.; Monaco, C.; Stocchi, P. The timescale and spatial extent of vertical tectonic motions in Italy: Insights from relative sea-level changes studies. Journal of the Virtual Explorer. **2010**, 36, doi:10.3809/jvirtex.2009.00255.
17. Antonioli, F.; Silenzi, S.; Vittori, E.; Villani, C. Sea level changes and tectonic mobility: precise measurements in three coastlines of italy considered stable during the last 125 kyrs. *Physics and Chemistry of the Earth*. **1999**, 24(4): 337–342.
18. Issel, A. Lembi fossiliferi quaternari e recenti osservati nella Sardegna meriodionale dal Prof. D. Lovisato. *Rendiconti dell'Accademia de Sciences. 1914*, 5a (23), 759e770.
19. Ulzega, A.; Ozer, A. Comptes-rendus de 1'Excursion Table Ronde sur le Tyrsrhénien de Sardaigne. *INQUA*. **1982**, Cagliari.
20. Ulzega, A.; Hearty, J. P. Geomorphology, Stratigraphy and Geochronology of late Quaternary marine deposits in Sardinia . 2. *Geomorph. N. F., Suppl. -Bd*. **1986**, 62, 119-129.
21. Cobby, D.M.; Mason, D.C.; Davenport, I.J. Image processing of airborne scanning laser altimetry data for improved river flood modelling. ISPRS Journal of Photogrammetry and Remote Sensing. **2001**, 56, 121–138, doi:10.1016/S0924-2716(01)00039-9.
22. EMODnet Bathymetry Viewing and Download Service. Available online: https://portal.emodnet-bathymetry.eu/ (accessed on 16 December 2020).
23. Global Mapper - All-in-one GIS Software Available online: https://www.bluemarblegeo.com/products/global-mapper.php (accessed on Apr 15, 2020).
24. Segre, A. G. Linee di riva sommerse e morfologia della piattaforma continentale relativa alla trasgressione marina versiliana. *Quaternaria*. **1968**, 11, 1-14.
25. Orrù, P.E.; Antonioli, F.; Lambeck, K.; Verrubbi, V. Holocene sea-level change in the Cagliari coastal plain (South Sardinia, Italy) – *Quaternaria Nova*. **2004**, VIII, 193-210.
26. Lodolo, E.; Galassi, G.; Spada, G.; Zecchin, M.; Civile, D.; Bressoux, M.; (2020) Post-LGM coastline evolution of the NW Sicilian Channel: Comparing high-resolution geophysical data with Glacial Isostatic Adjustment modeling. PLoS ONE 15(2): e0228087. https://doi.org/10.1371/journal.pone.0228087
27. Peirano, A.; Morri, C.; Bianchi, C.N.; Aguirre, J.; Antonioli, F.; Calzetta, G.; Carobene, L.; Mastronuzzi, G.; Orru' P. The Mediterranean coral Cladocora coespitosa: a Proxy for past climate fluctuations?. *Global and Planetary Change*. **2004**, 841 2003. https://doi.org/10.1016/S0921-8181(03)00110-3.
28. Orrù, P.E.; Antonioli, F.; Hearty, P. J.; Radtke, U. Chronostatigarphic confirmation of MIS 5 age of a baymouth bar at Is Arenas (Cagliari, Italy). *Quaternary International.* **2011**,232 169-178. 10.1016/j.quaint.2010.04.031
29. Deiana, G.; Meleddu, A.; Paliaga, E.; Todde, S.; Orrù, P. Continental slope geomorphology: Landslides and pockforms of Southern Sardinian margin (italy). Geogr. Fis. Dinam. Quat. 2016, 39, 129–136. Doi: 10.4461/GFDQ2016.39.12
30. Solinas E.; Orrù P.E. (2006), Santa Gilla: spiagge sommerse e frequentazioni di epoca punica, in Aequora, pontoq, jam, mare... Mare uomini e merci nel Mediterraneo antico, Atti del Convegno Internazionale (Genova, 9-10 dicembre 2004), a cura di B. M. Giannattasio, G.; Canepa, L.: Grasso, E.; Piccardi, Estratto, pp. 1-4
31. Antonioli, F.; Anzidei, M.; Auriemma, R.; Gaddi, D.; Furlani, S.; Lambeck, K.; Orrù P.E.; Solinas E.; Gaspari, A.; Karinja, S.; Kovacic, V.; Surace, L. Sea level change during Holocene from Sardinia and northeastern Adriatic from archaeological and geomorphological data. *Quaternary Science Review*. **2007**,26, 2435-2458. https://doi.org/10.1016/j.quascirev.2007.06.022

Preprints (www.preprints.org) | NOT PEER-REVIEWED | Posted: 13 August 2021

32. Buosi, C.; Del Rio, M.; Orrù, P.E.; Pittau, P.; Scanu, G.; Solinas, E.; Sea level changes and past vegetation in the Punic period (5the4th century BC): Archaeological, geomorphological and palaeobotanical indicators (South Sardinia e West Mediterranean Sea). *Quaternary International.* **2017**, 439, 141-157. https://doi.org/10.1016/j.quaint.2016.07.005
33. Lecca, L.; Carboni, S. The Tyrrhenian section of San Giovanni di Sinis (Sardinia): Stratigraphic record of an irregular single high stand. *Rivista Italiana di Paleontologia e Stratigrafia*. **2007**, 113 (3), 509-523.
34. Carboni, S.; Lecca, L.; Hilaire-Marcel, C.; Ghaleb, B. MIS 5e at San Giovanni di Sinis (Sardinia, Italy): Stratigraphy, U/Th dating and "eustatic" inference. *Quaternary International*, **2014**. 328–329, 21-30, https://doi.org/10.1016/j.quaint.2013.12.052.
35. 34 Segre, A.G. Il Quaternario del Golfo di Terranova Pausania (Olbia) e la sua fauna malacologica. Boll. Serv. Geol. d'Italia. **1954**, vol.76, pag. 45-73.
36. Porqueddu, A.; Antonioli, F.; D'Oriano, R.; Gavini, V.; Trainito, E.; Verrubbi, V. Relative sea level change in Olbia Gulf (Sardinia, Italy), a historically important Mediterranean harbour. *Journal of Quaternary International.* **2011**, 232(1-2):21-30
37. Blanc, A. C. Stratigrafia del Canale Mussolini nell'Agro Pontino. Società Toscana Scienze Naturali.**1935**, 54, 52-56.
38. Blanc, A.C.; Segre A.G. ; Le Quaternaire du Mont Circe´. Livret Guide 'Excursion au Mont Circe'', *IV International Meeting INQUA*. **1953**. 23–108, Roma
39. Segre, A.G. Nota sui rilevamenti eseguiti nel Foglio 158 Latina della Carta Geologica d'Italia. *Boll. Serv. Geol. It*. **1957**, 73, 569-584, Roma.
40. Blanc, A.C.; De Vries M.; Follieri M.;. A first C14 date for the Würm I chronology on the italian coast. *Quaternaria*. **1957**, 4, 83–89.
41. Durante, S. Sul Tirreniano e la malacofauna della Grotta del Fossellone (Circeo). Quaternaria. **1975**, 18: 331–347.
42. Hearty P.J.; Dai-Pra G.;. Aminostratigraphy of Quaternary marine deposits in the Lazio region of central Italy. In: Ozer, A., Vita-Finzi, C. (Eds.), *Dating Mediterranean Shorelines, Zeitschrift Fuer Geomorphologie*, Supplementband. **1986**, 62, 131–140.
43. Dai Pra, G.; Arnoldus-Huyzendveld A. Lineamenti stratigrafici, morfologici e podologici della fascia costiera dal fiume Tevere al fiume Astura (Lazio, Italia Centrale). *Geologica Romana*. **1984,** 23: 1–12.
44. Antonioli, F.; Dai Pra, G.; Hearty, P.J. I sedimenti quaternari nella fascia costiera della Piana di Fondi (Lazio meridionale). *Bollettino della Societa Geologica Italiana*.**1988**,107: 491–501.
45. Barbieri M.; Carrara, C.; Castorina, F.; Dai Pra G.; Esu, D.; Gliozzi, E.; Paganin, G.; Sadori, L. Multidisciplinary study of Middle–Upper Pleistocene deposits in a core from the Piana Pontina (central Italy). *Giornale di Geologia*. **1999**, 61: 47–73.
46. Nisi, M. F.; Antonioli, F.; Dai Pra, G.; Leoni, G.; Silenzi, S. Coastal deformation between the Versilia and the Garigliano plains (Italy) since the last interglacial stage. *Quaternary Sci*.. **2003**, 18, 709–721. https://doi.org/10.1002/jqs.803
47. Bigi, G.; Casentino, D.; Parlotto, M. Modello litostratigrafico-strutturale della Regione Lazio. Scala 1:250.000. Regione Lazio, Università. degli Studi di Roma "La Sapienza", Dip. Scienze della Terra. **1988**.
48. Serva, L. ; Brunamonte, F. Subsidence in the Pontina Plain, Italy. *Bull. Eng. Geol. Env.* **2007**, 66: 125–134. doi 10.1007/s10064-006-0057-y
49. Blanc, AC. Una spiaggia pleistocenica a Strombus bubonius presso Palidoro (Roma). *Rendiconti Accademia Nazionale Lincei*. **1936**, 23: 200–204.
50. Farina, S. Late Pleistocene-Holocene mammals from "Canale delle Acque Alte (Canale Mussolini)" (Agro Pontino, Latium) *B. Soc. Paleontol. Ital*. **2011**, 50, pp. 11-22
51. Arnoldus-Huyzendveld, A., Perotto, C., Sarandrea, P. I suoli della provincia di Latina. Carta, database e applicazioni, Roma: Gangemi Editore. **2009**
52. Liboni, A. Affioramento fossile con malacofauna tra il Quadrato e Casale Nuovo.Borgo Sabotino - Latina), *Studi per l'ecologia del Quaternario*. **1983**, 131–134.
53. Hearty, P.J. An inventory of Last Interglacial (sensu lato) age deposits from the Mediterranean Basin: a study of Isoleucine epimerization and U-series dating. Z. *Geomorph. N.F.,* Suppl.-bd. 1986, 62, 51-69
54. Antonioli, F.; Lo Presti,V.; Rovere, A.; Ferranti, L.; Anzidei, M.; Furlani, S.; Mastronuzzi, G.; Orrù, P.E.; Scicchitano, G.; Sannino, G.; Spampinato, C.R.; Pagliarulo, R.; Deiana, G.; de Sabata, E.; Sanso, P.; Vacchi, M.; Vecchio A. Tidal notches in Mediterranean Sea: a comprehensive analysis. *Quat. Sci. Rev.* **2015**,119, pp. 66-84. https://doi.org/10.1016/j.quascirev.2015.03.016
55. Hearty, P.J.; Rovere, A.; Sandstrom ,M.R.; O'Leary, M.J.; Roberts, D.; Raymo, M.E. Pliocene - Pleistocene Stratigraphy and Sea - Level Estimates, Republic of South Africa With Implications for a 400 ppmv CO2 World. Paleoceanography and Paleoclimatology. 2020, 357. https://doi.org/10.1029/2019PA003835
56. Rovere, A.; Pappalardo, M.; Richiano, S.M., Aguirre, M.L.; Sandstrom, M.R. An Early Pliocene relative sea level record from Patagonia (Argentina) *Nature Geoscience*. **2020**,
57. Gilford, D. M.; Ashe, E.L.; DeConto, R.M.; Kopp, R.E.; Pollard, D.; Rovere, A. Could the Last Interglacial constrain projections of future Antarctic ice mass loss and sea-level rise?. *Journal of Geophysical Research: Earth Surface*. **2020**,125. https://doi.org/10.1029/2019JF005418
58. Ashkenazy, Y.; I Eisenman I. Gildor H.The effect of Milankovitch variations in insolation on equatorial seasonality. *Journal of Climate.* **2010**, 23. 6133-6142. doi.org/10.1175/2010JCLI3700.1
59. Kirkby J. Cosmic rays and climate. European organization for nuclear research. CERN Report -PH-EP/**2008**-005. 31 pp.
60. Manara, V.; Brunetti, M.; Celozzi, A.; Maugeri, M.; Sanchez, L.; Wild, M. Detection of dimming/brightening in Italy from homogenized all-sky and clear-sky surface solar radiation records and underlying causes (1959–2013). *Atmos. Chem. Phys*. **2016**. 16, 11145–11161. doi.org/10.5194/acp-16-11145-2016

Preprints (www.preprints.org) | NOT PEER-REVIEWED | Posted: 13 August 2021

61. Marsh, G.E.. Interglacials, Milankovitch Cycles, Solar Activity, and Carbon Dioxide. *Journal of Climatology*. **2014,** 345482, 7 pages. dx.doi.org/10.1155/2014/345482
62. Smulsky, J.J. A New Theory of Change in the Insolation of the Earth over Millions of Years against Marine Isotope Stages. *Atmospheric and Oceanic Physics*. **2020**, 56, No. 7, 721–747. doi: 10.1134/S0001433820070087